

MISIMO:

A Multi-Input Single-Inductor Multi-Output Energy Harvester Employing Event-Driven MPPT Control to Achieve 89% Peak Efficiency and a 60,000x Dynamic Range in 28nm FDSOI

Sally Safwat Amin and Patrick P. Mercier

University of California, San Diego, La Jolla, CA, USA





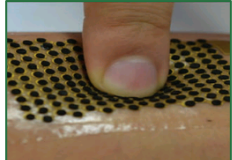


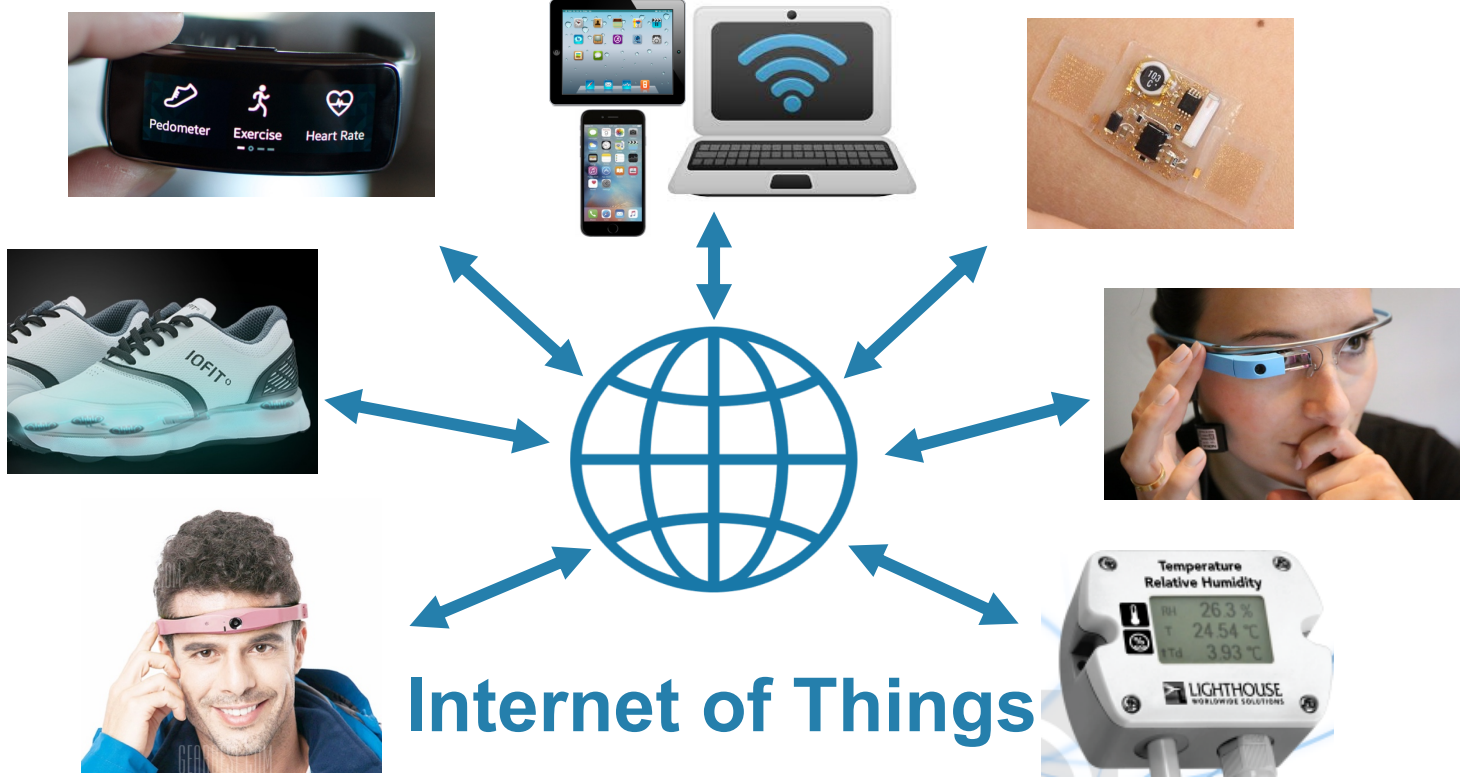
UC San Diego

ISSCC 2018



Energy Harvesting for Powering Wearable and IoT Devices

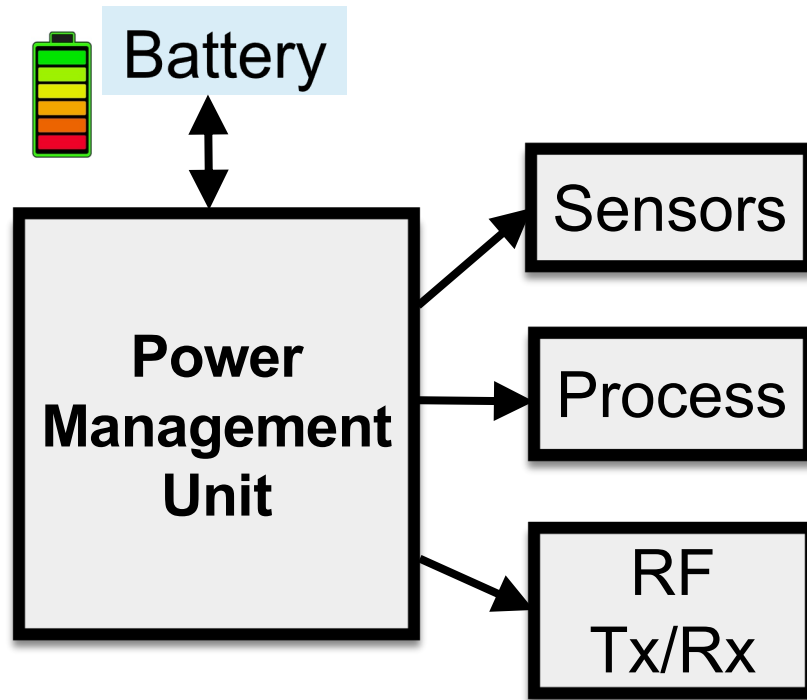
- Light 
- Heat 
- RF 
- motion 
- Biofuel 



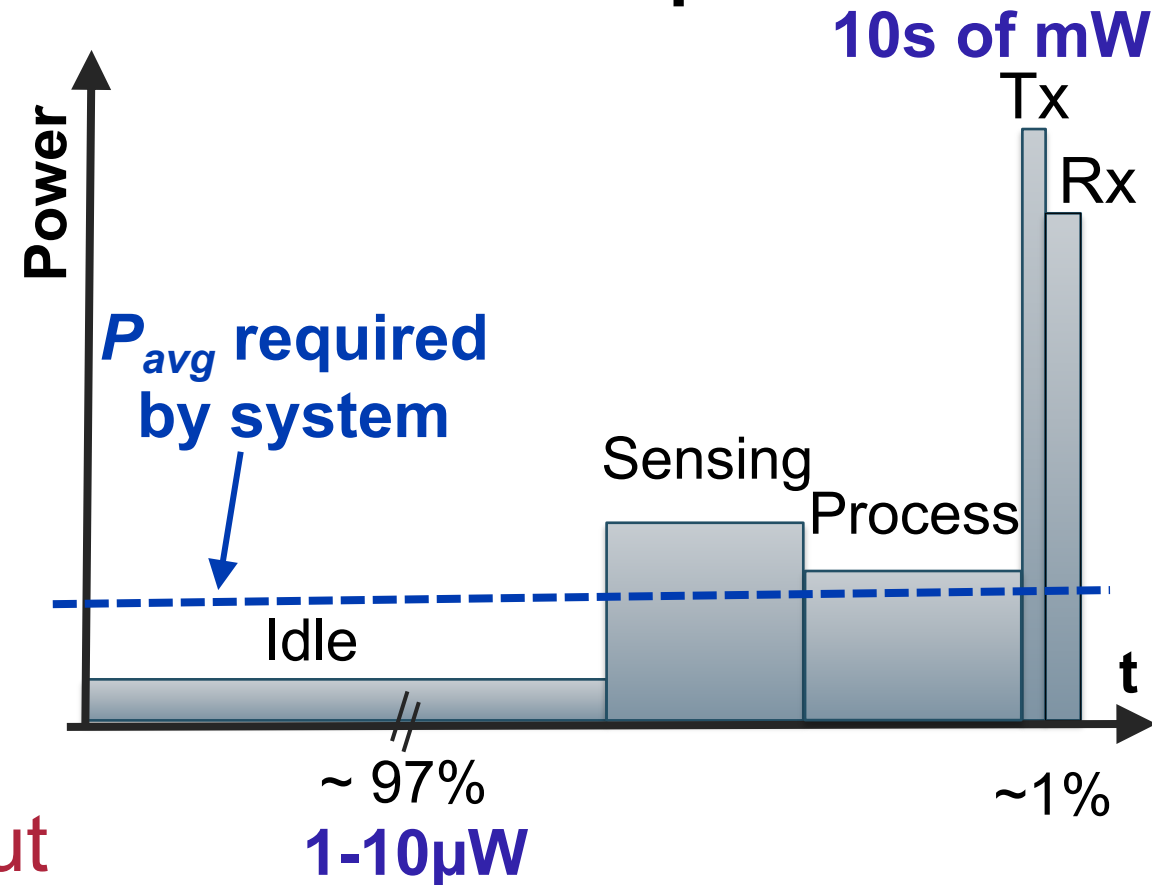
Enable small wearable/IoT devices from ambient energy
– No battery re-charging/replacement

Wireless Sensor Device Power Demand Pattern

Wireless sensor device



Power demand pattern

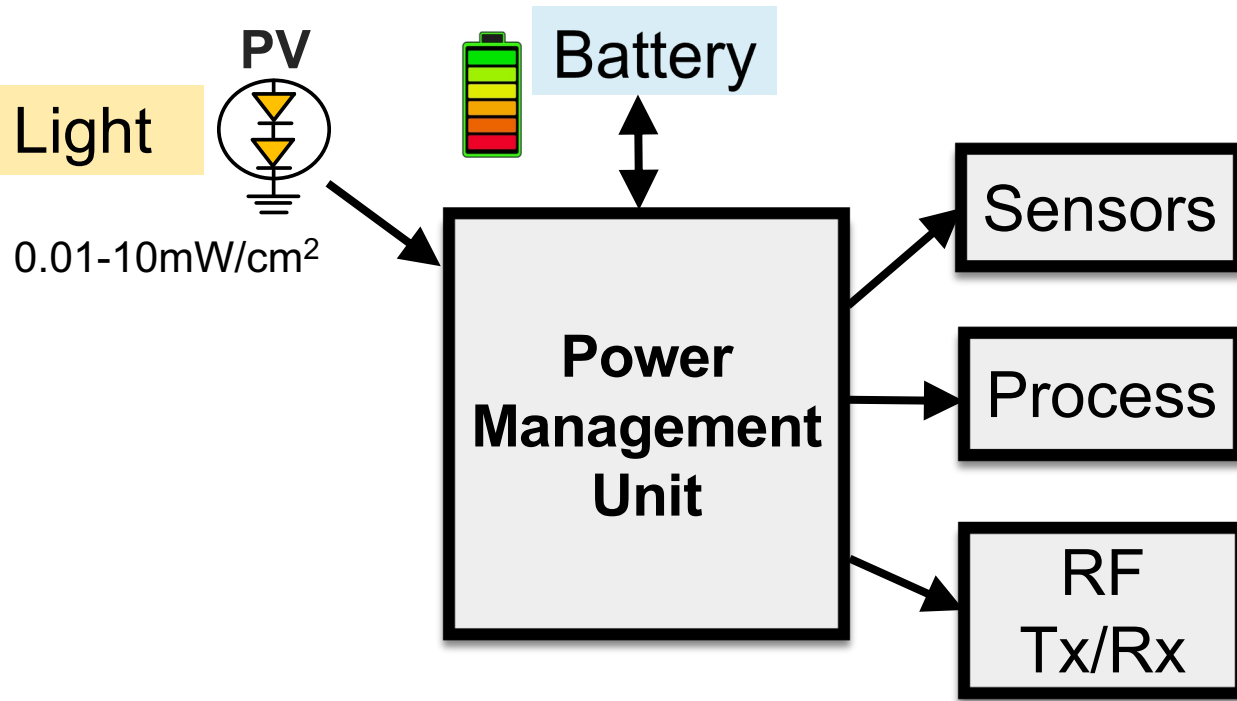


Multi-Output

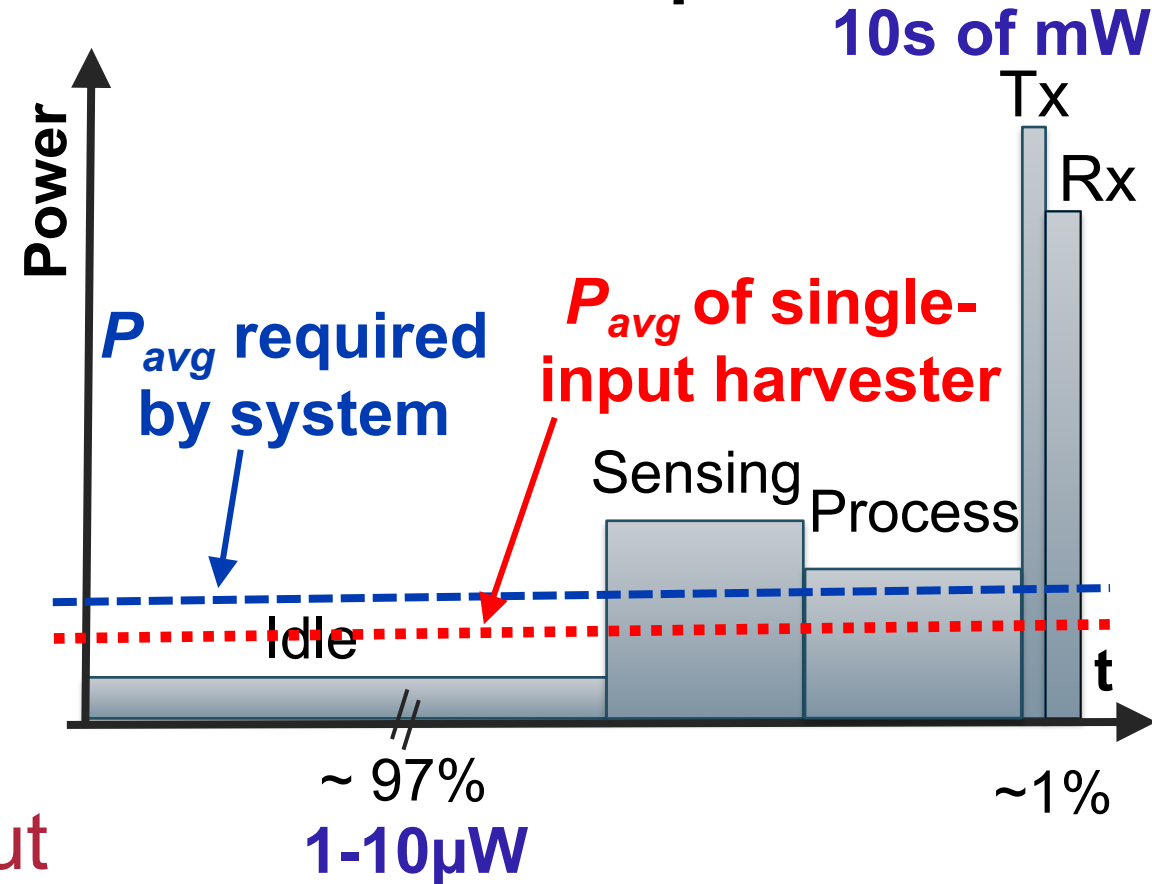
$\geq 97\%$ idle state, $\leq 3\%$ active state

Energy Harvesting Promise in IoT

Wireless sensor device



Power demand pattern



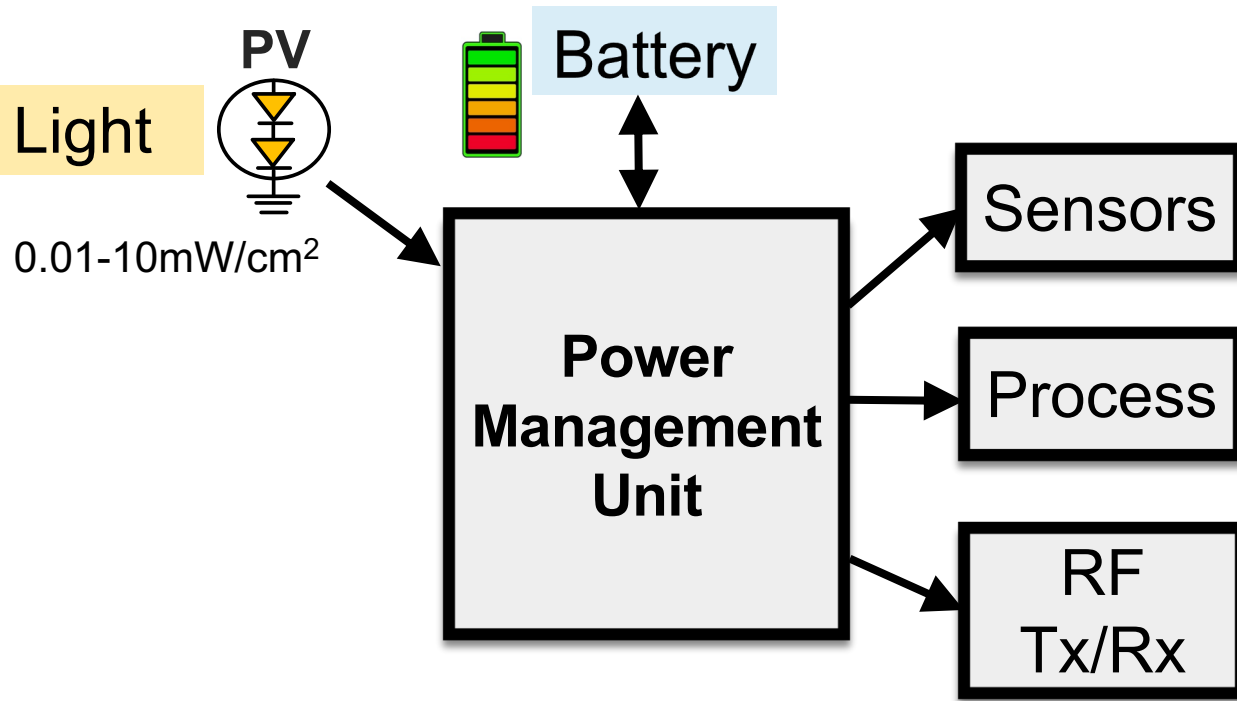
Single-Input

Multi-Output

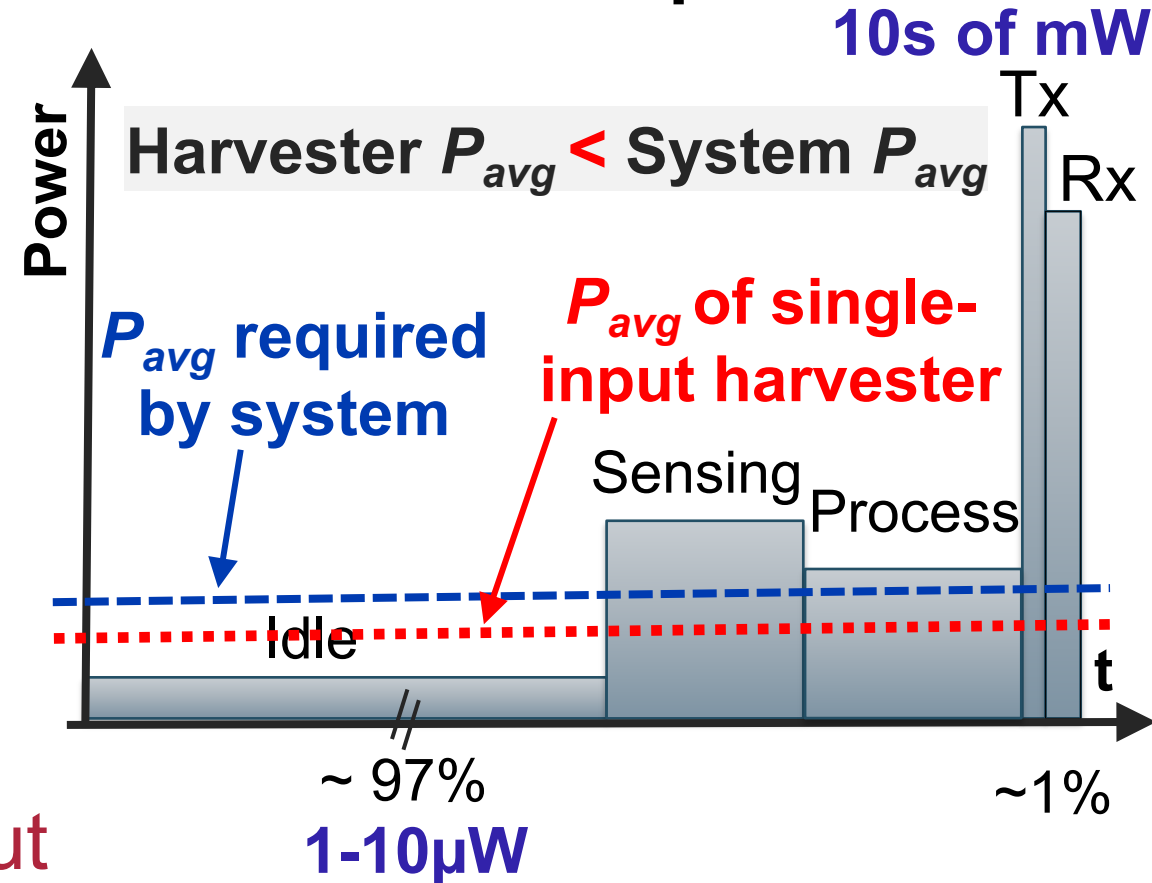
Energy harvesting can extend battery life

Single-Input Harvesting Limitation

Wireless sensor device



Power demand pattern



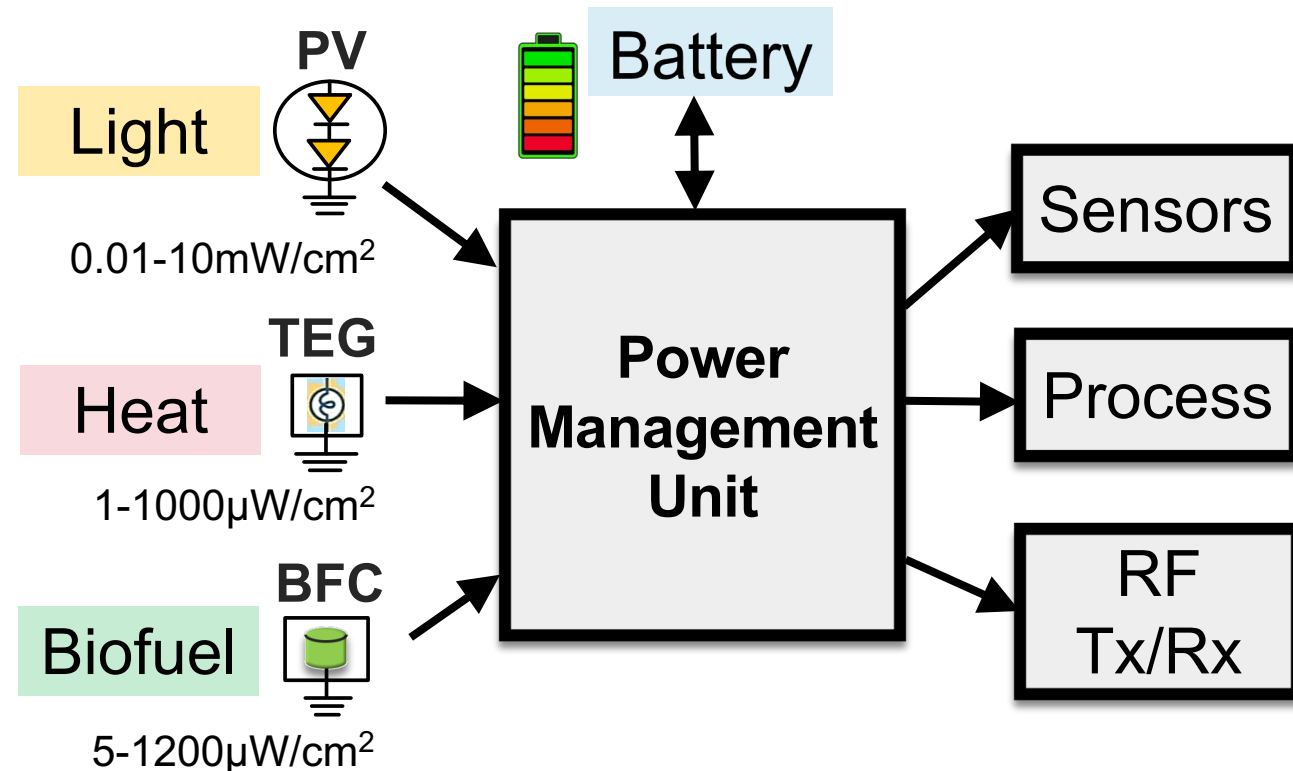
Single-Input

Multi-Output

Power available from harvester is low and stochastic

Power Aggregation for Autonomous Operation

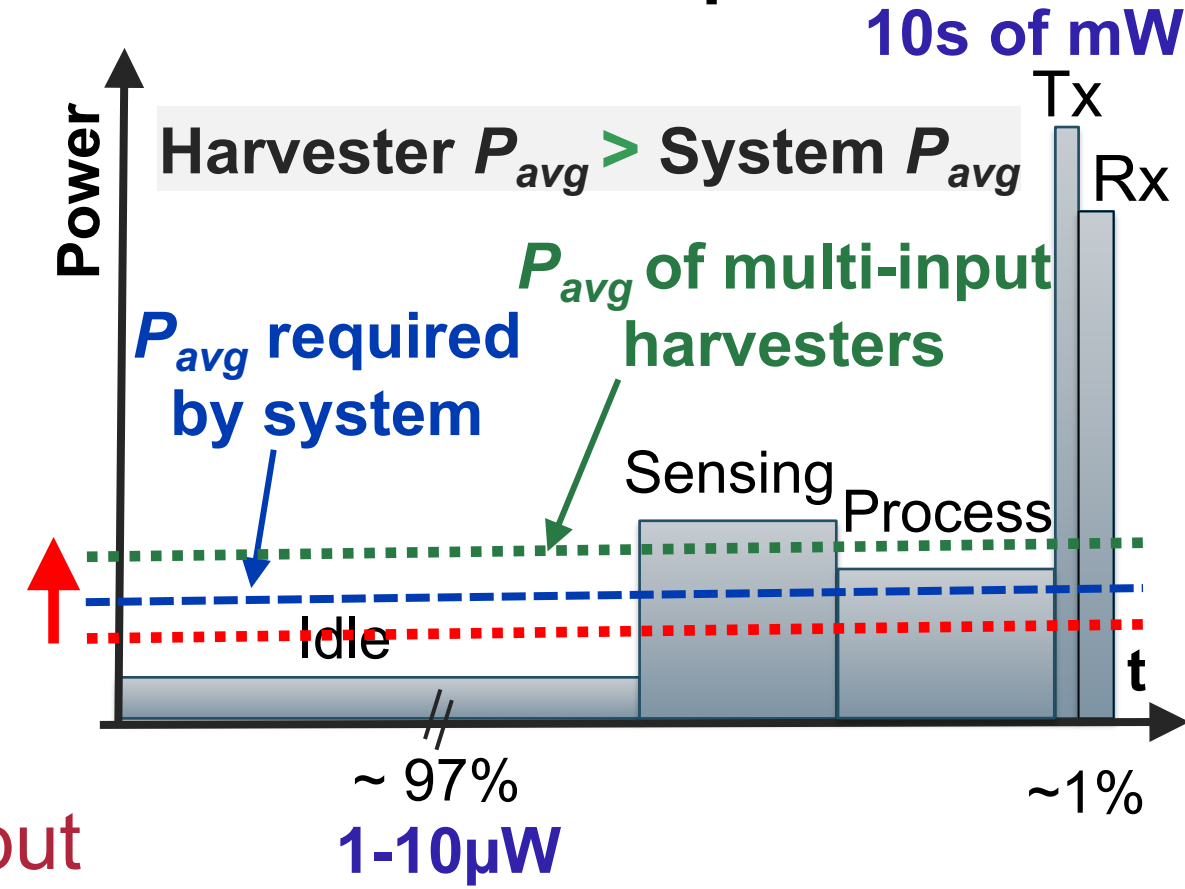
Wireless sensor device



Multi-Input

Multi-Output

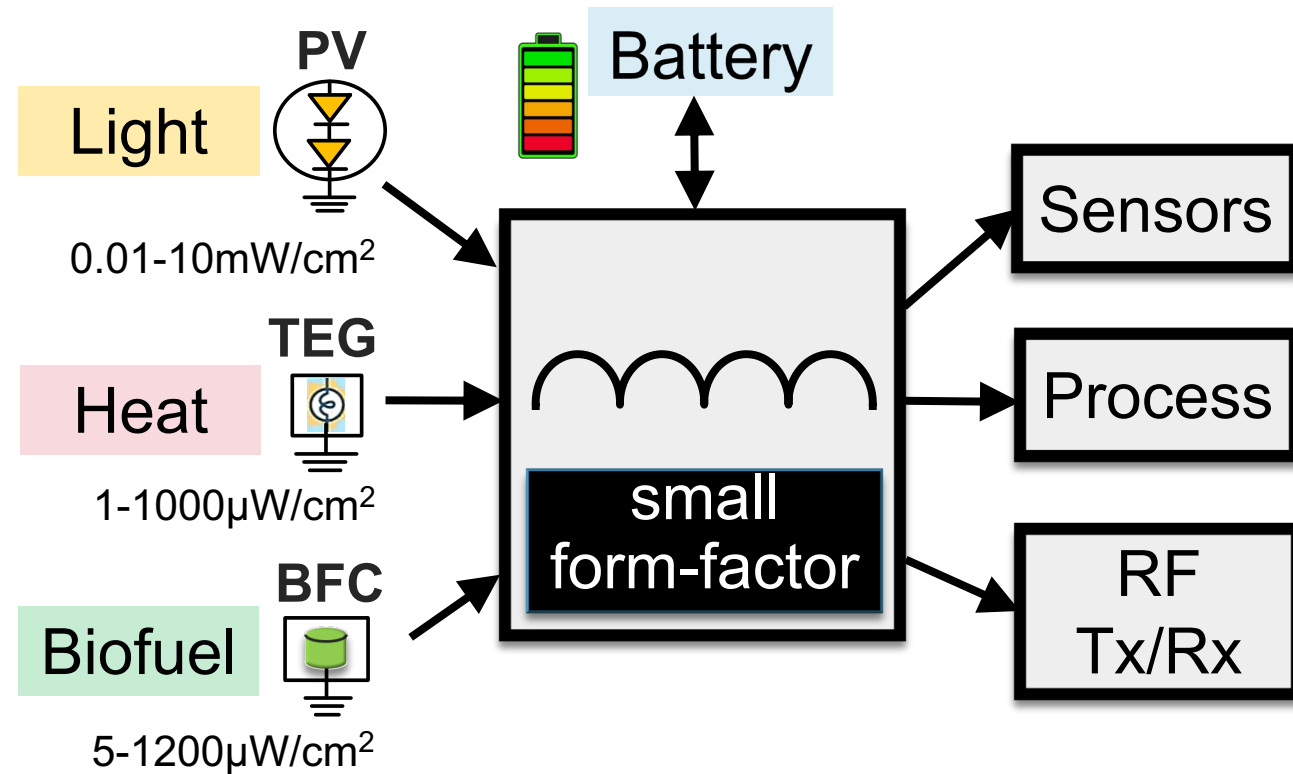
Power demand pattern



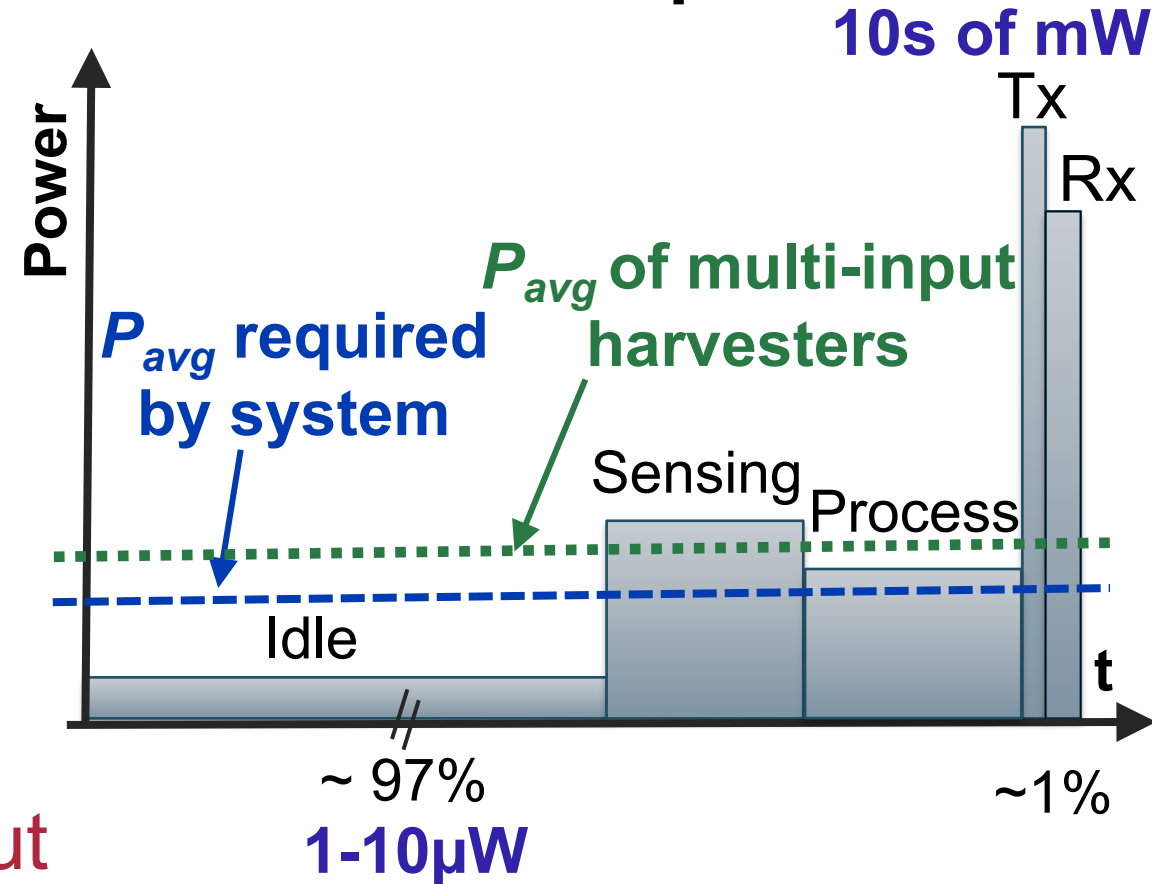
Multi-input harvesting increases harvester P_{avg}

Small Form-Factor MISIMO for Powering IoT Devices

Wireless sensor device



Power demand pattern

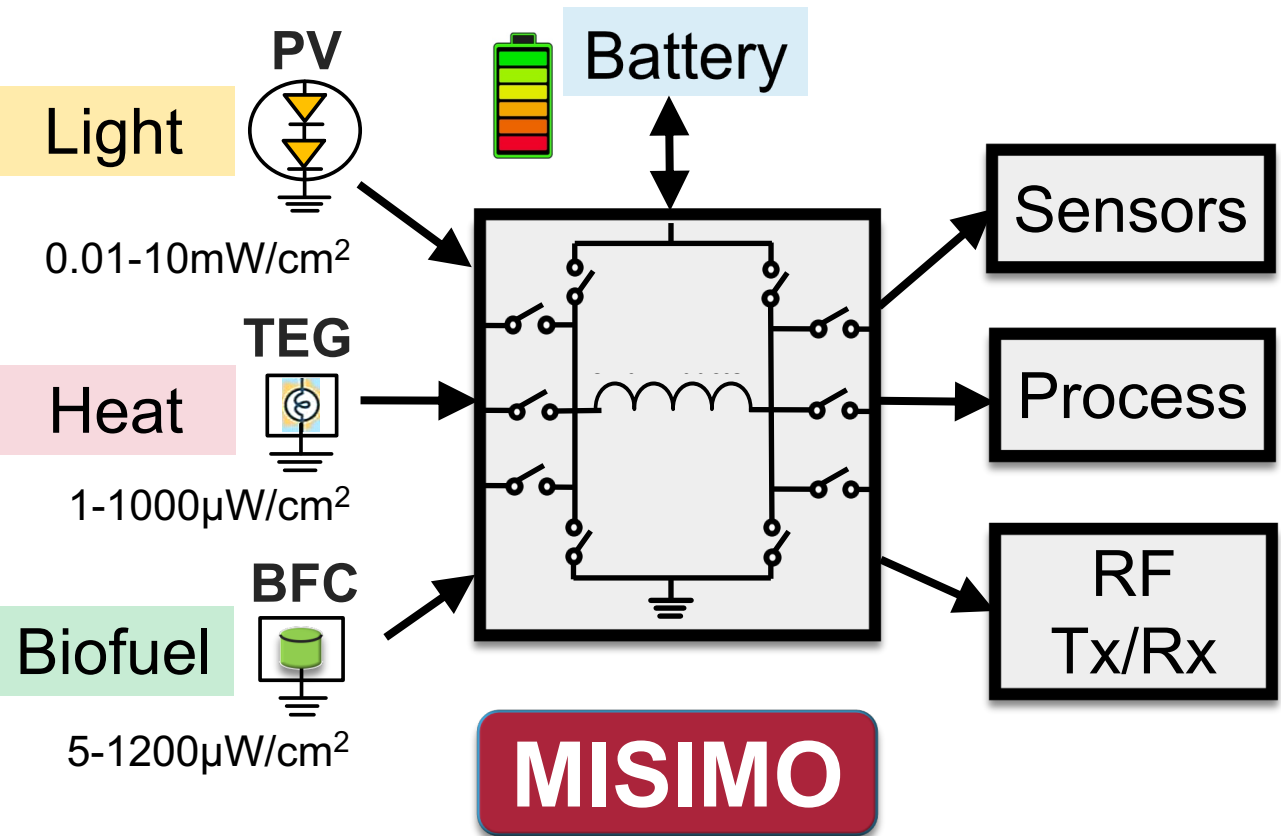


Multi-Input Single-Inductor Multi-Output

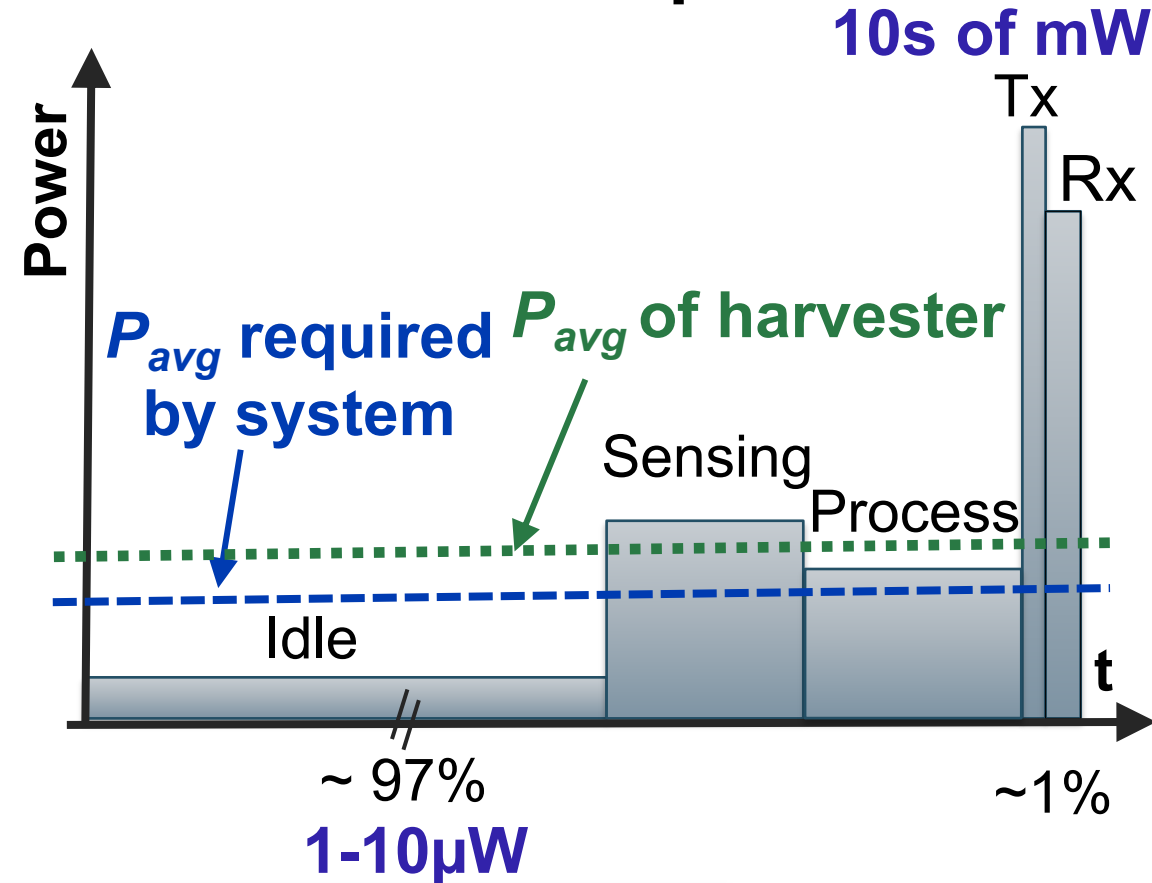
MISIMO

MISIMO Dynamic Switching Capability

Wireless sensor device



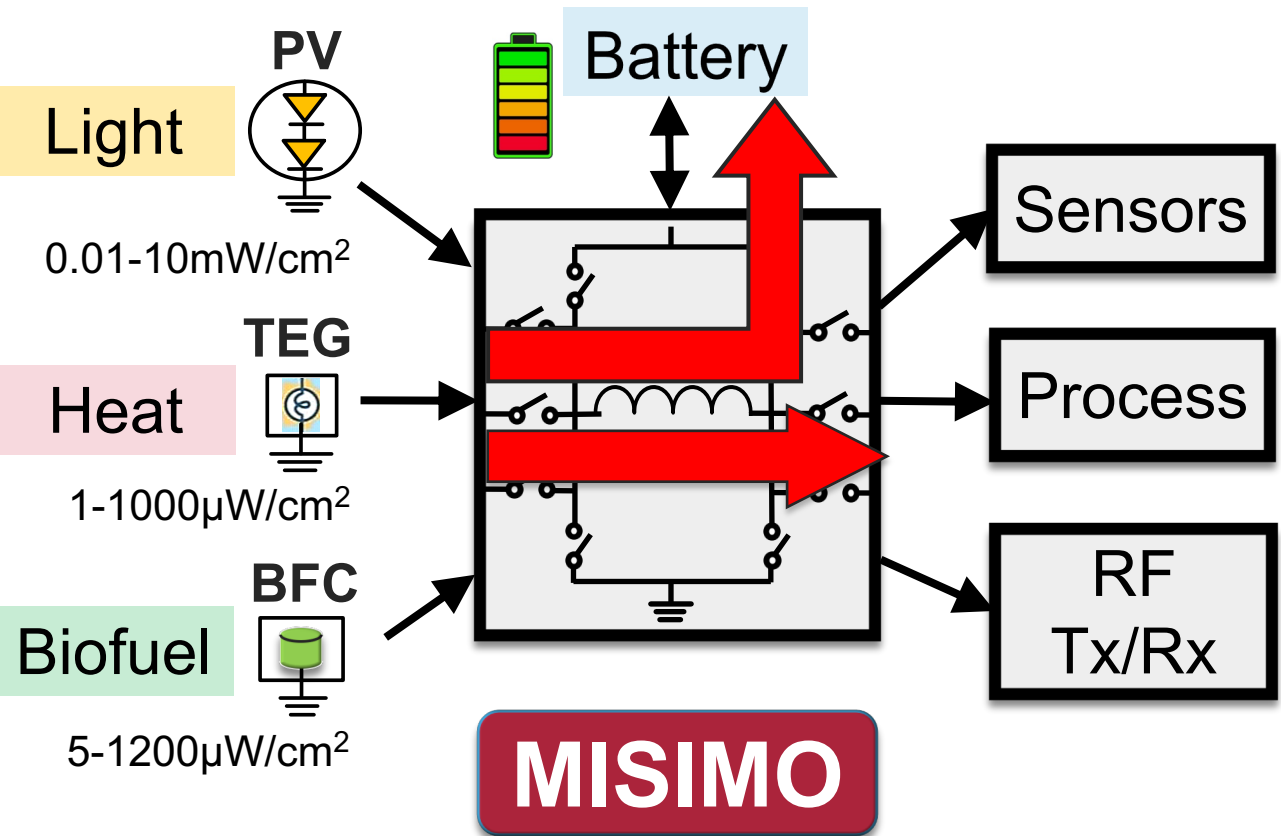
Power demand pattern



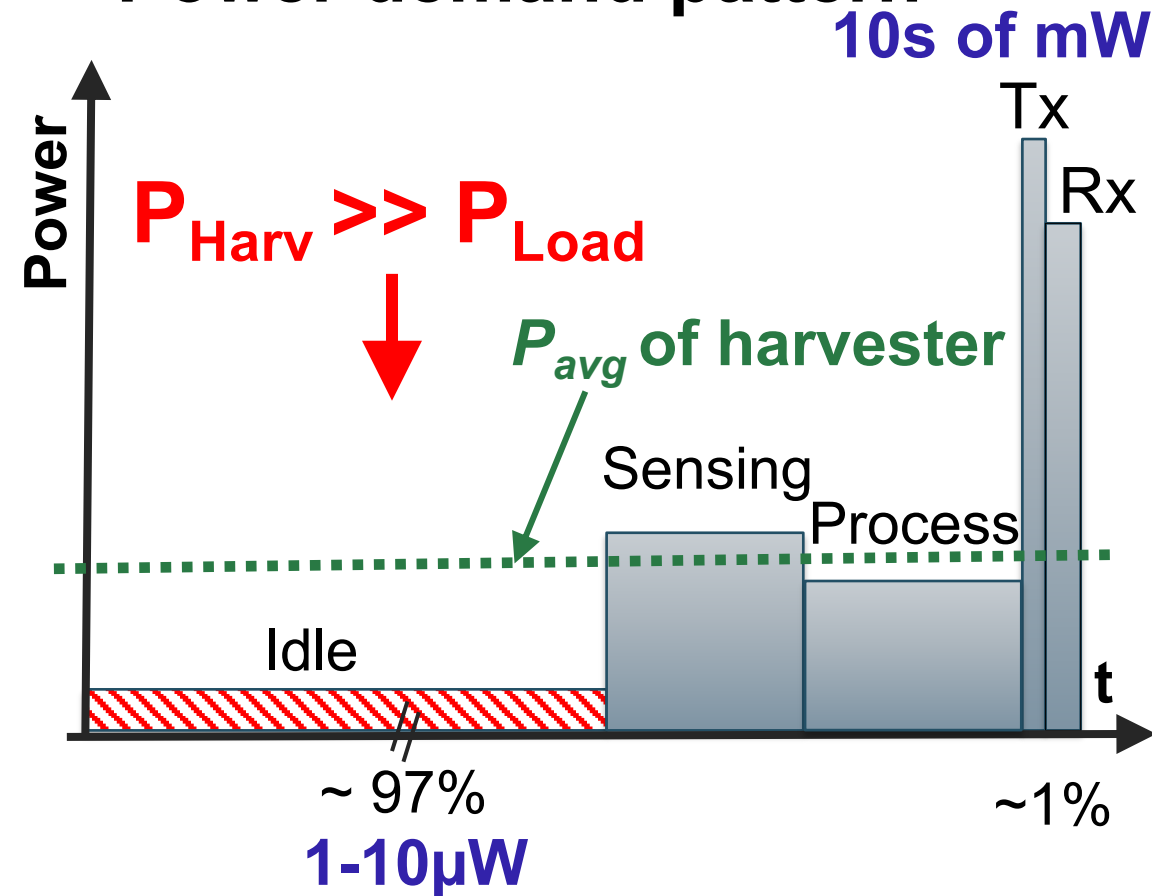
MISIMO dynamically switches between different configurations based on harvester/load conditions

MISIMO Dynamic Switching Capability

Wireless sensor device

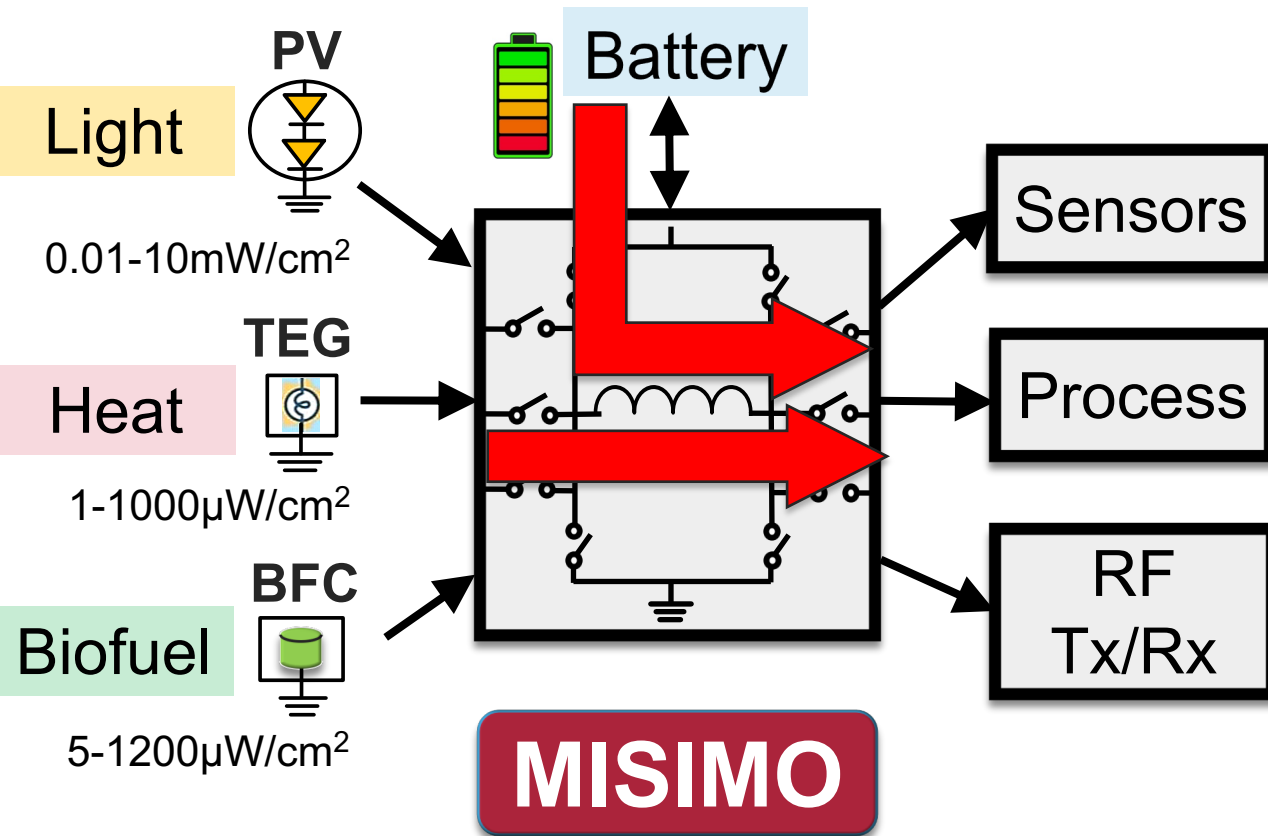


Power demand pattern

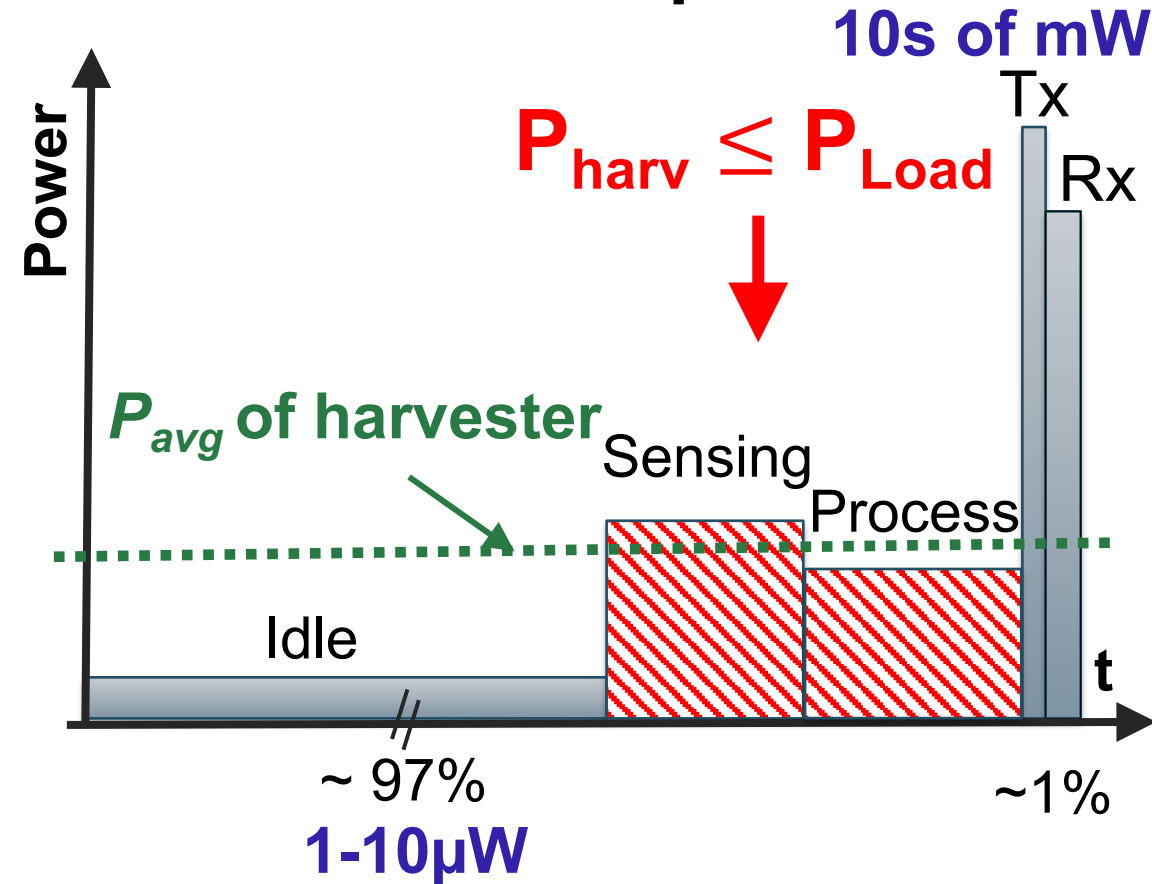


MISIMO Dynamic Switching Capability

Wireless sensor device

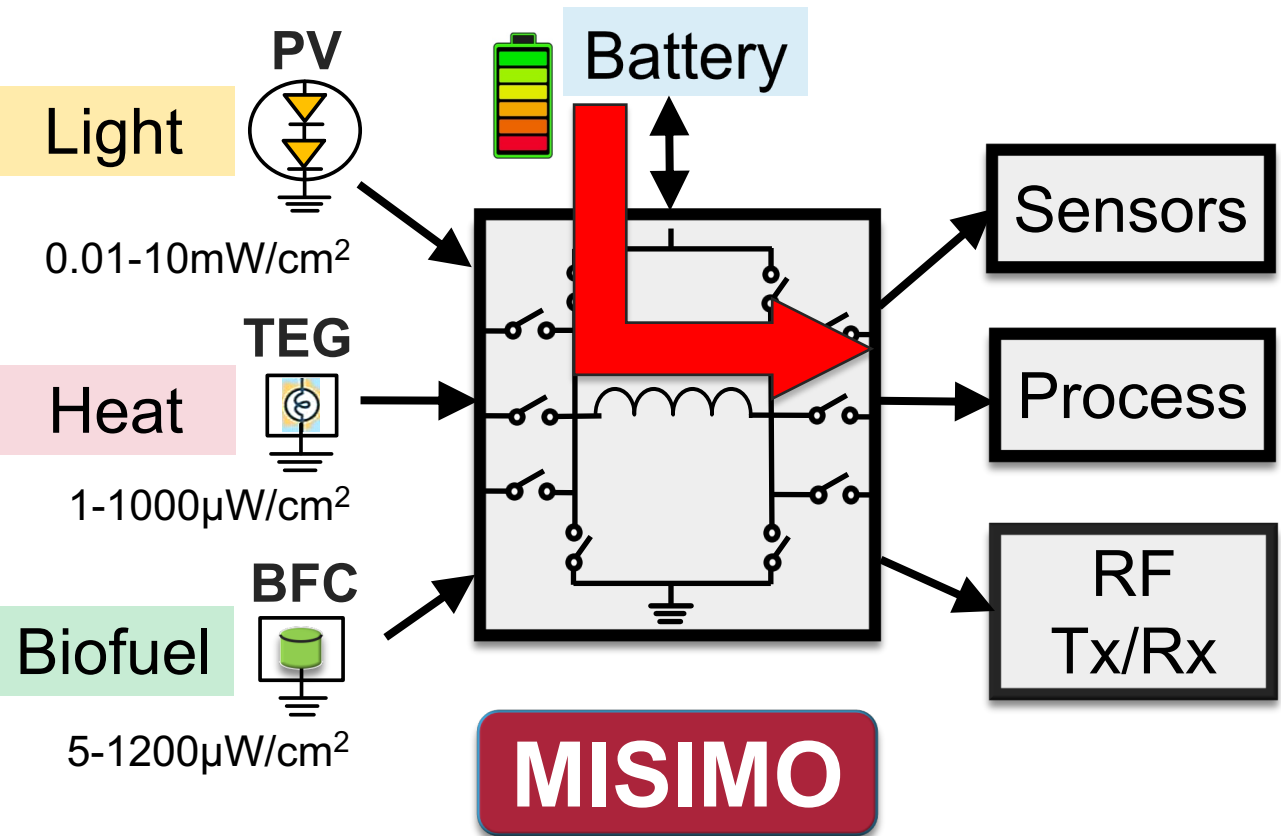


Power demand pattern

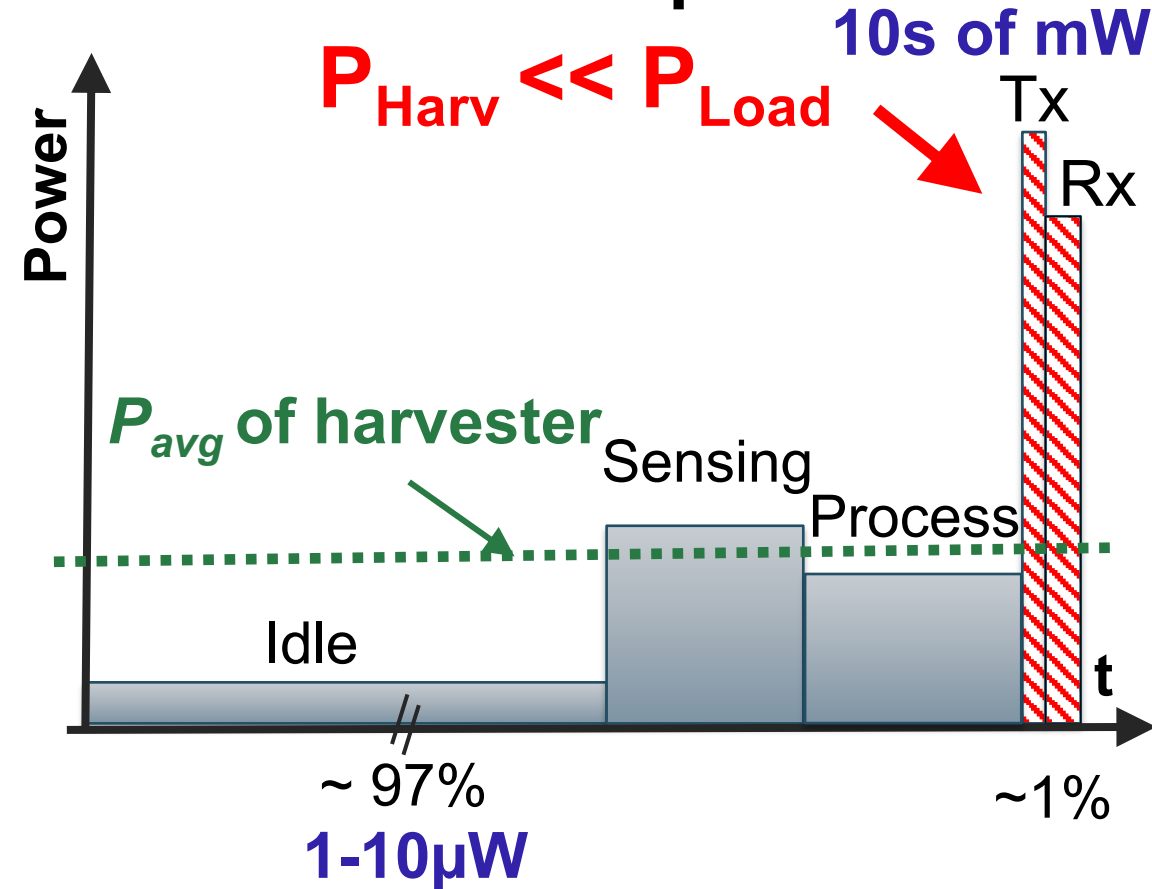


MISIMO Dynamic Switching Capability

Wireless sensor device



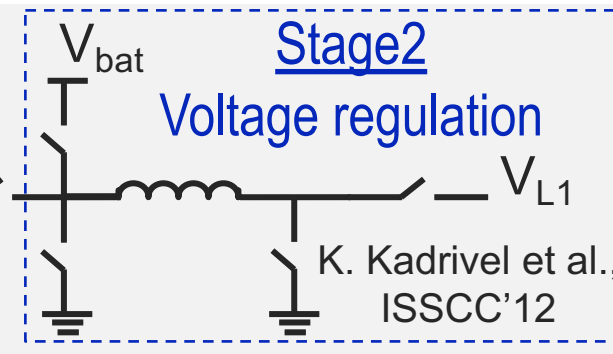
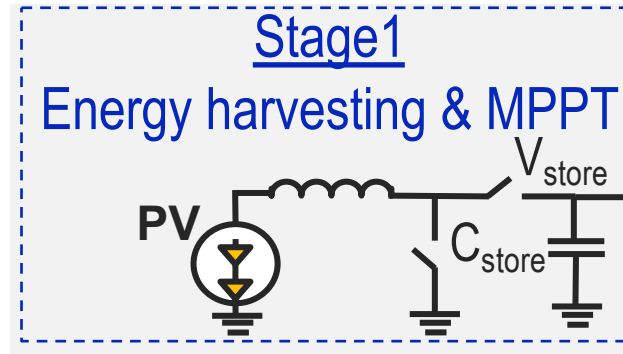
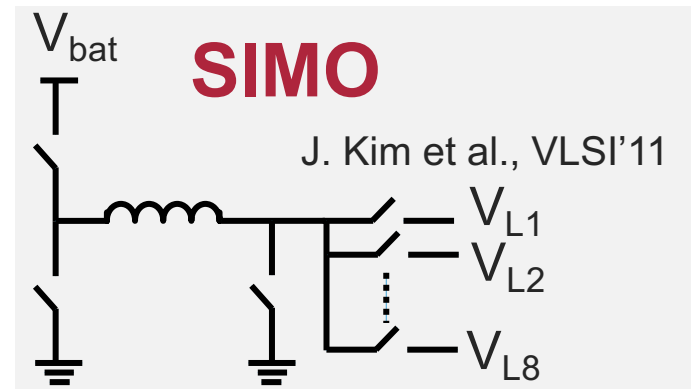
Power demand pattern



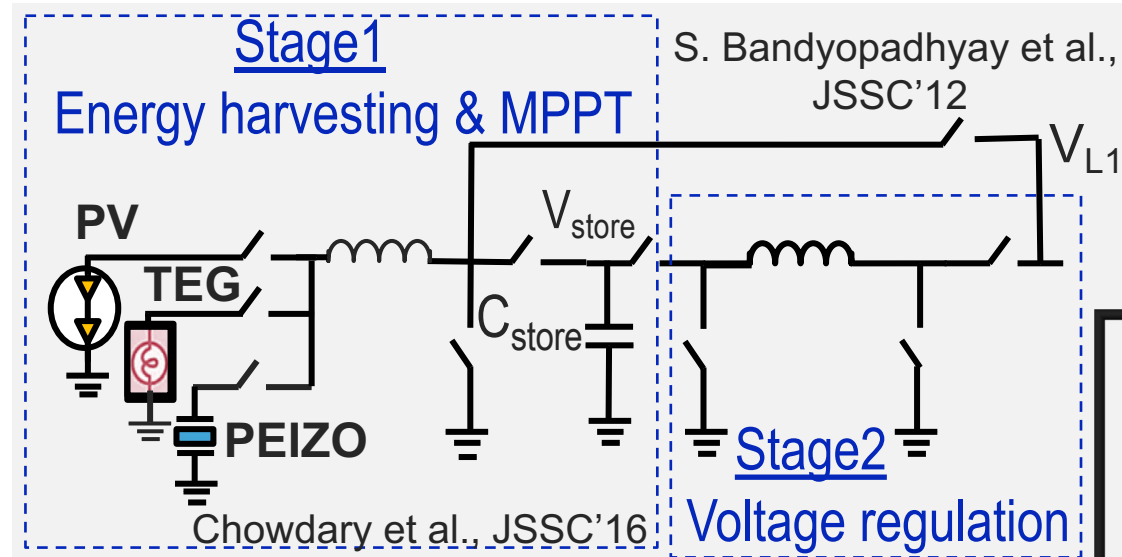
Outline

- State-of-the-Art and Single-Inductor Challenges
- Decoupling Source MPPT and Load Regulation
- Circuit Techniques for Wide Dynamic Range
- Measurement Results
- Conclusion

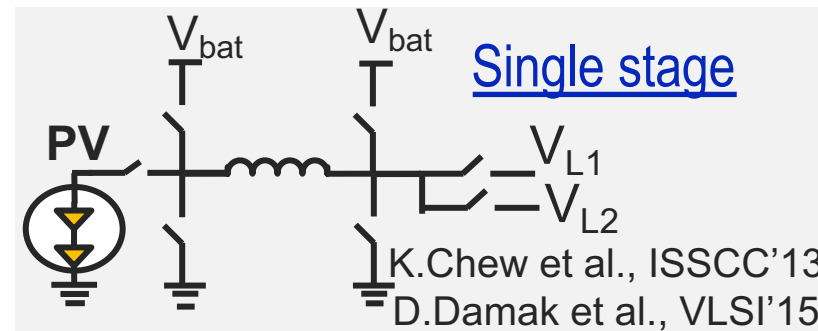
Towards Small Form-Factor MISIMO



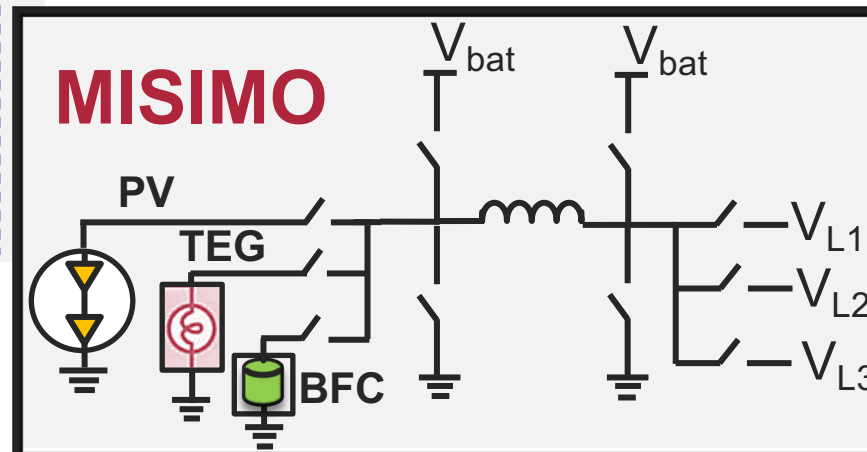
- Single input
- Single output
- Cascaded losses



- + Multiple inputs
- Cascaded losses
- Single output

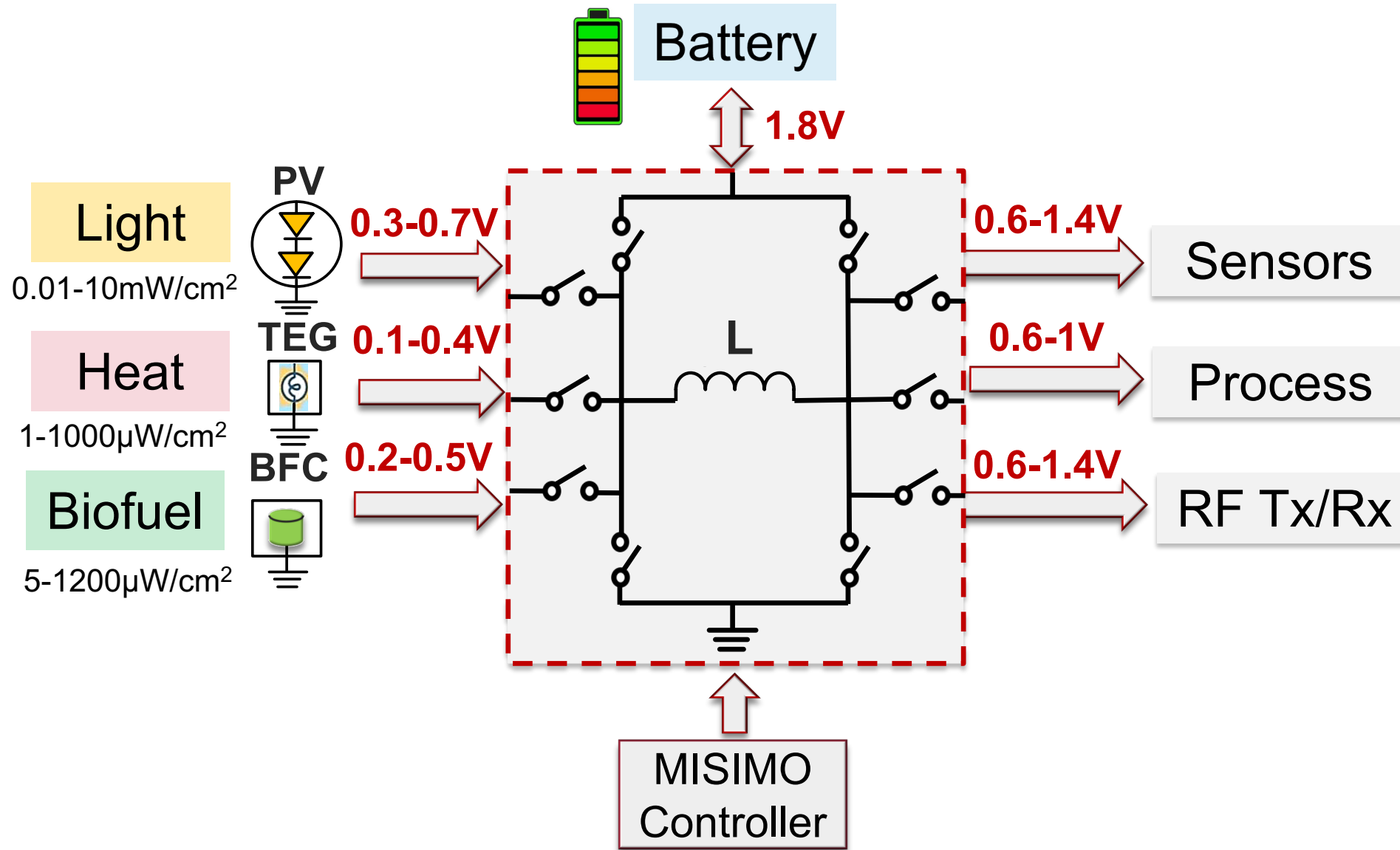


- + No cascaded losses
- + Multiple outputs
- Single input



- + No cascaded losses
- + Multiple inputs
- + Multiple outputs

MISIMO Goals and Challenges



MISIMO Goals and Challenges

Decouple source MPPT & load regulation sharing 1 inductor



Battery

1.8V

High end-to-end efficiency across wide power range

Light
0.01-10mW/cm²



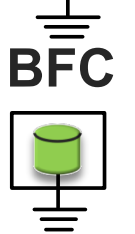
0.3-0.7V

Heat
1-1000μW/cm²



0.1-0.4V

Biofuel
5-1200μW/cm²



0.2-0.5V

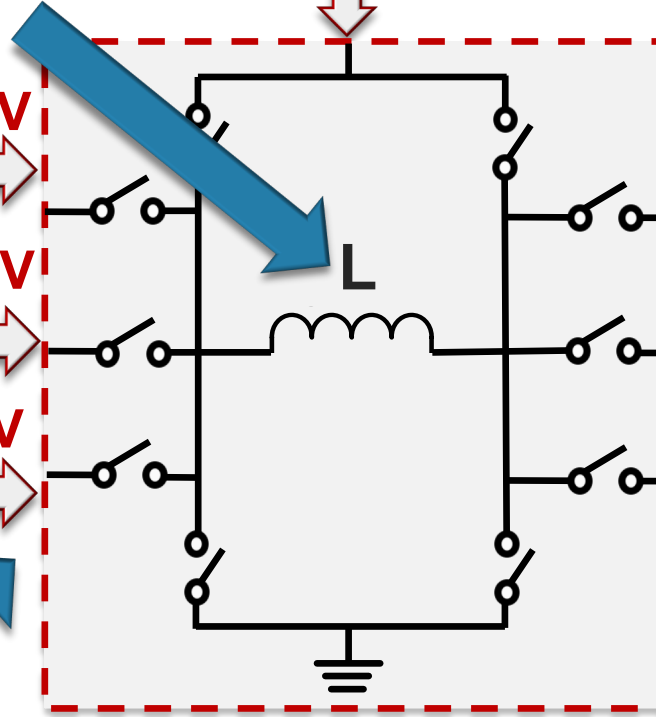
Simultaneous MPPT across all sources

Ultra low power controller with low quiescent power



MISIMO Controller

Independent regulation of all loads with a wide DR



0.6-1.4V

Sensors

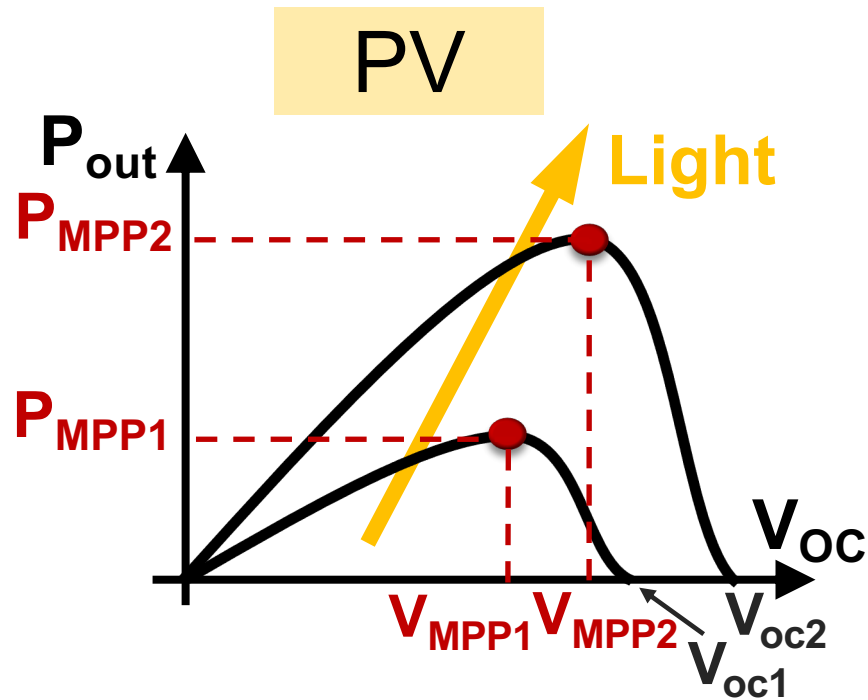
0.6-1V

Process

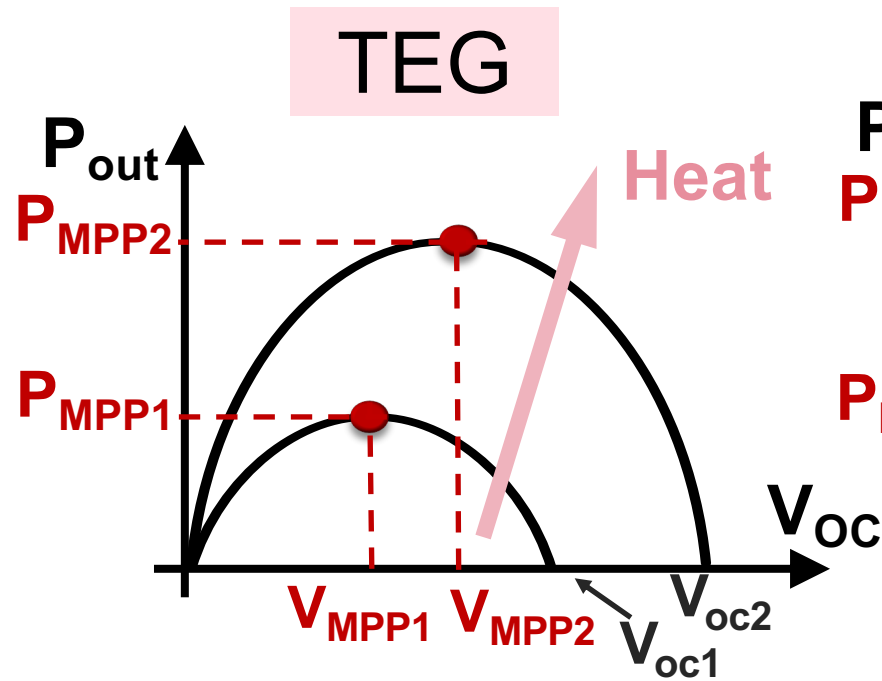
0.6-1.4V

RF Tx/Rx

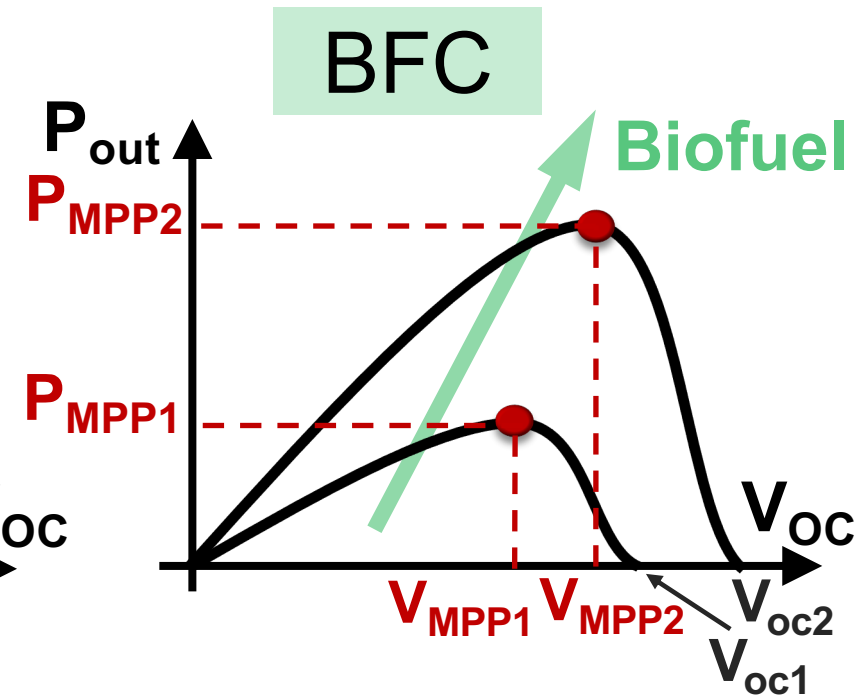
Fractional Open Circuit Voltage (VOC) MPPT



$$V_{MPP-PV} \approx 0.75 V_{OC}$$



$$V_{MPP-TEG} = 0.5 V_{OC}$$



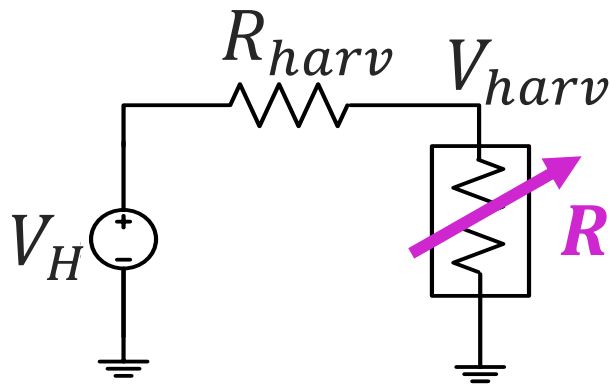
$$V_{MPP-BFC} \approx 0.6 V_{OC}$$

$$V_{MPP} = K V_{OC}$$

Generated by fractional VOC
sample and hold circuit

For MPPT: Input voltage is regulated around V_{MPP}

Hysteresis Comparator for 2-D MPPT



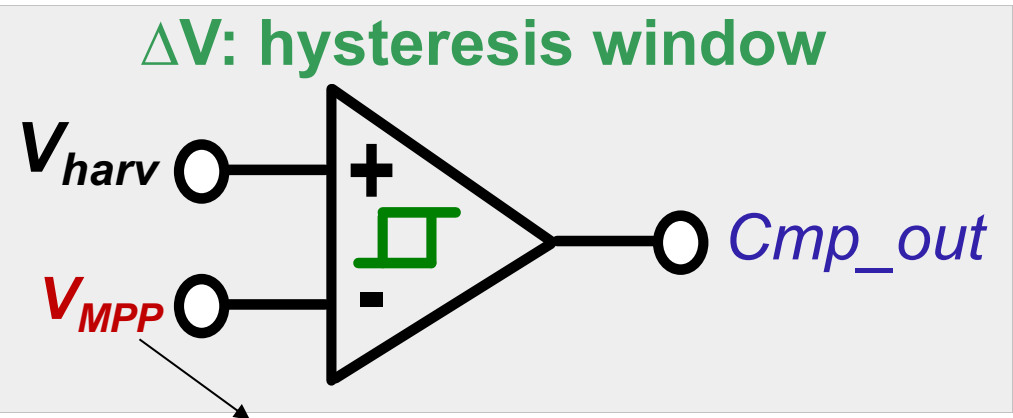
Adaptive to the available harvester energy

$$R_{conv} = \frac{2LT_{sw}}{T_{\phi 1}^2}$$

set for MPPT

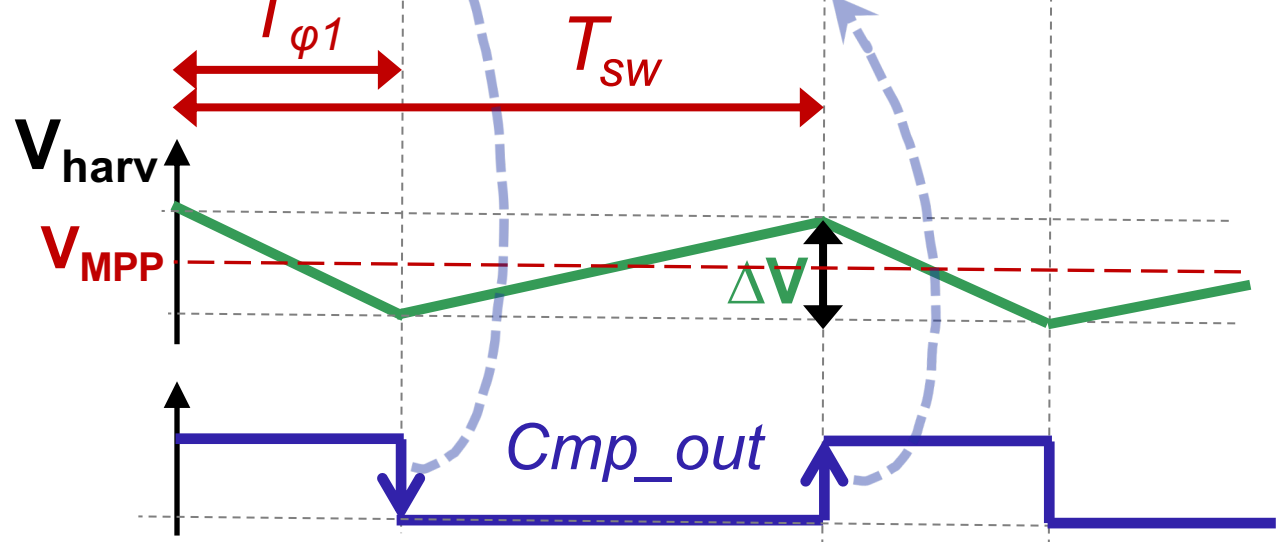
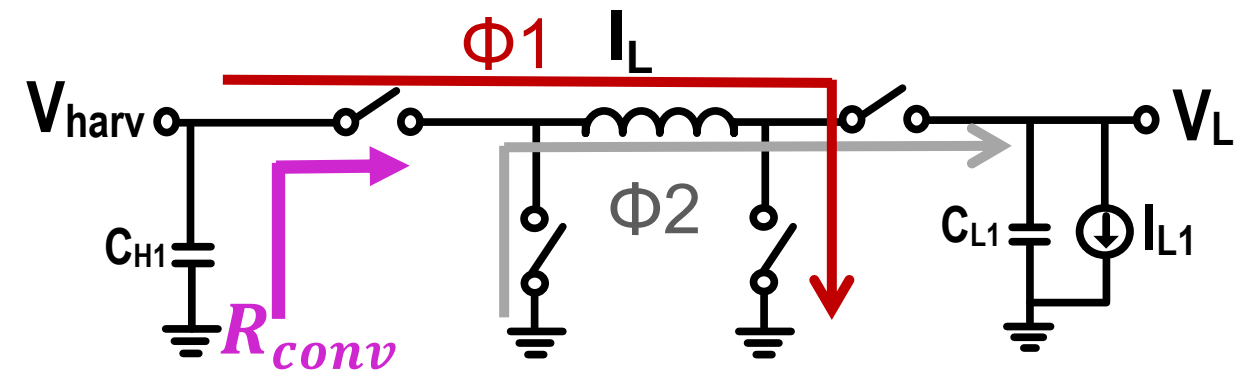
For MPPT

$$\begin{cases} R_{conv} = R_{harv} \\ V_{harv} = V_{MPP} \end{cases}$$

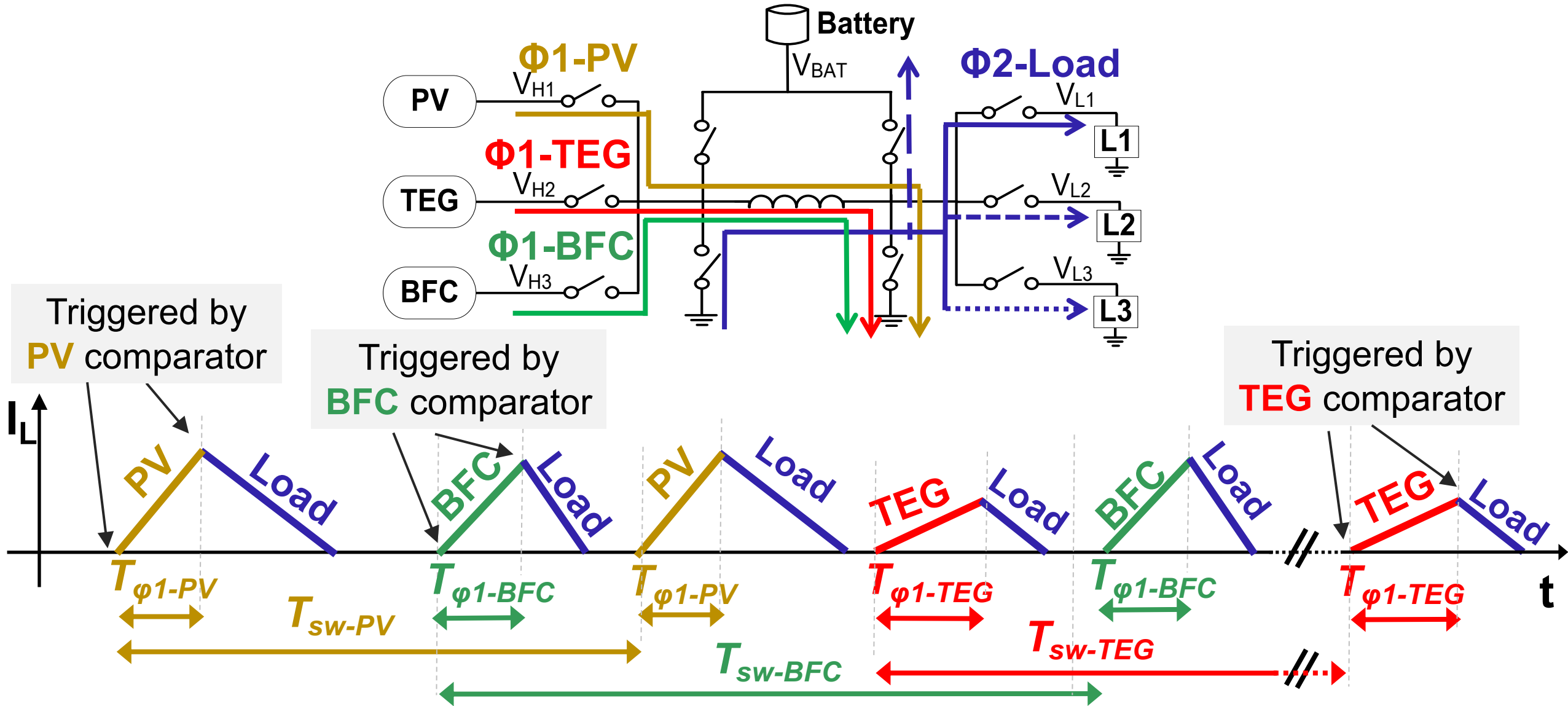


ΔV : hysteresis window

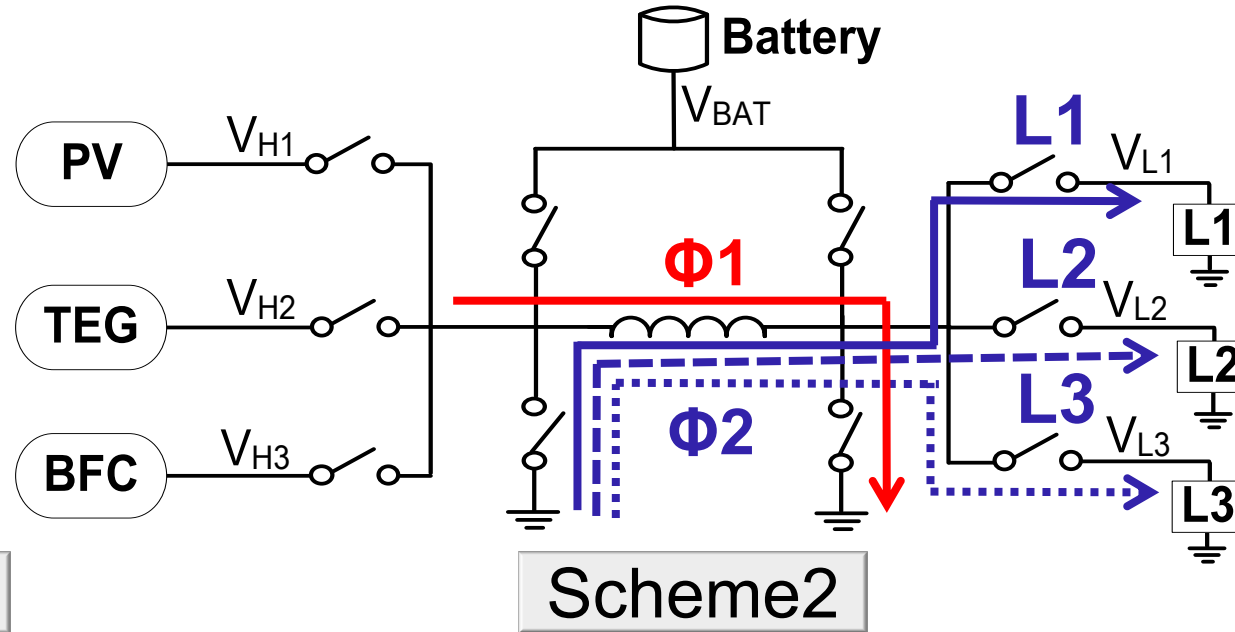
set by FVOC



Time-Shared Inductor for Multi-Input Harvesting

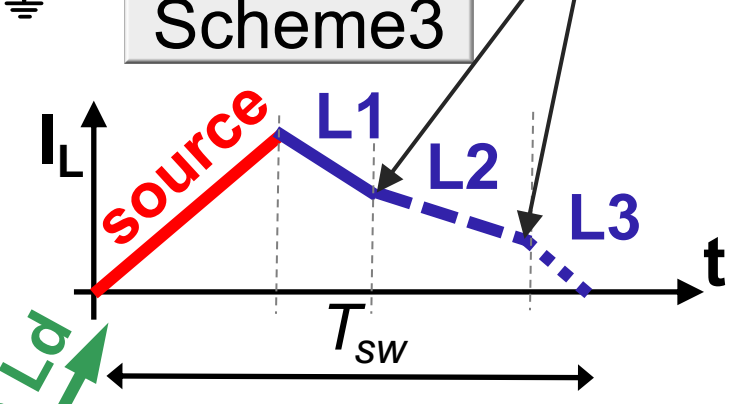
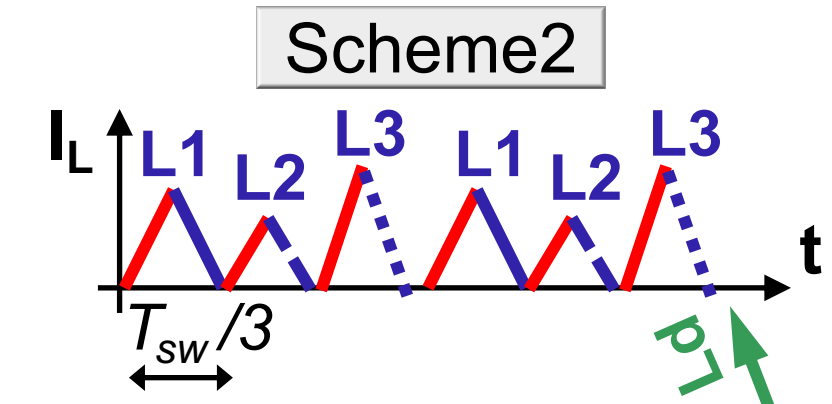
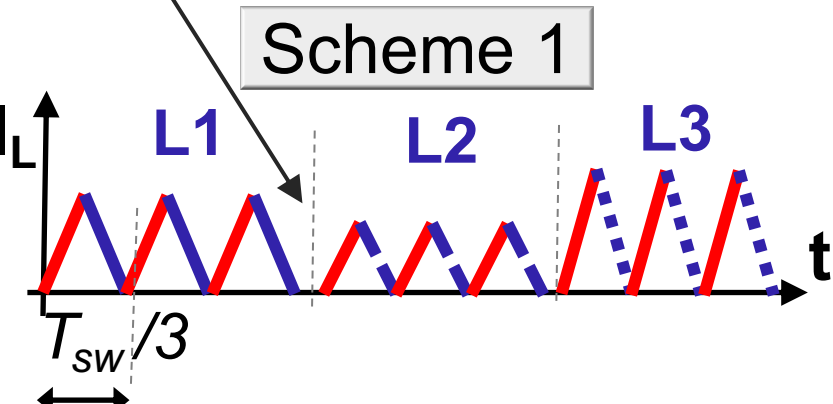


Inductor Switching Schemes for Load Regulation



L1 got sufficient energy

Triggered by load Hysteresis comparator



- High switching losses
- High voltage droop

- High switching losses
- + Low voltage droop

- + Low switching losses

MISIMO

D. Ma et al., JSSC'03

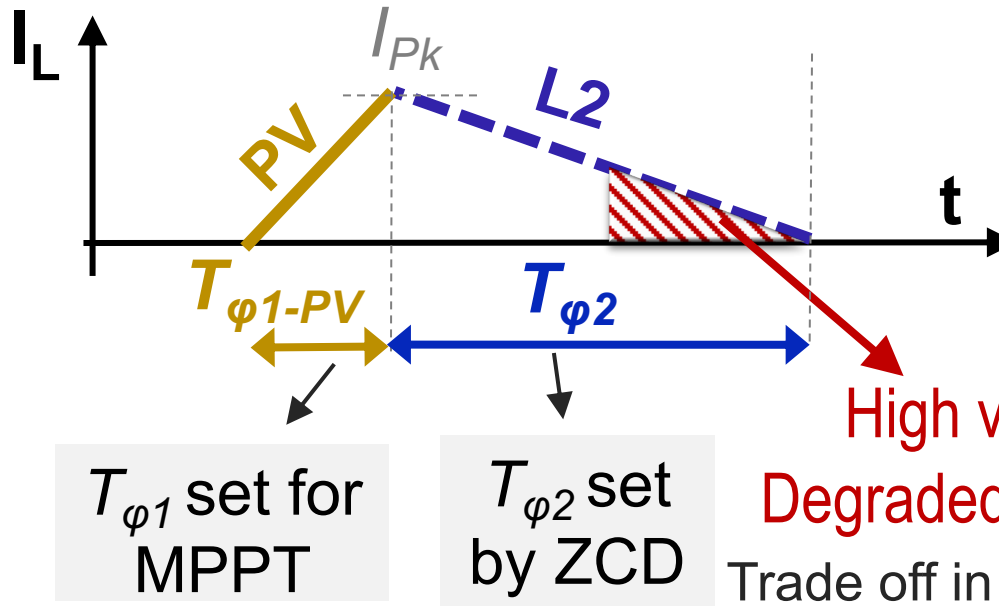
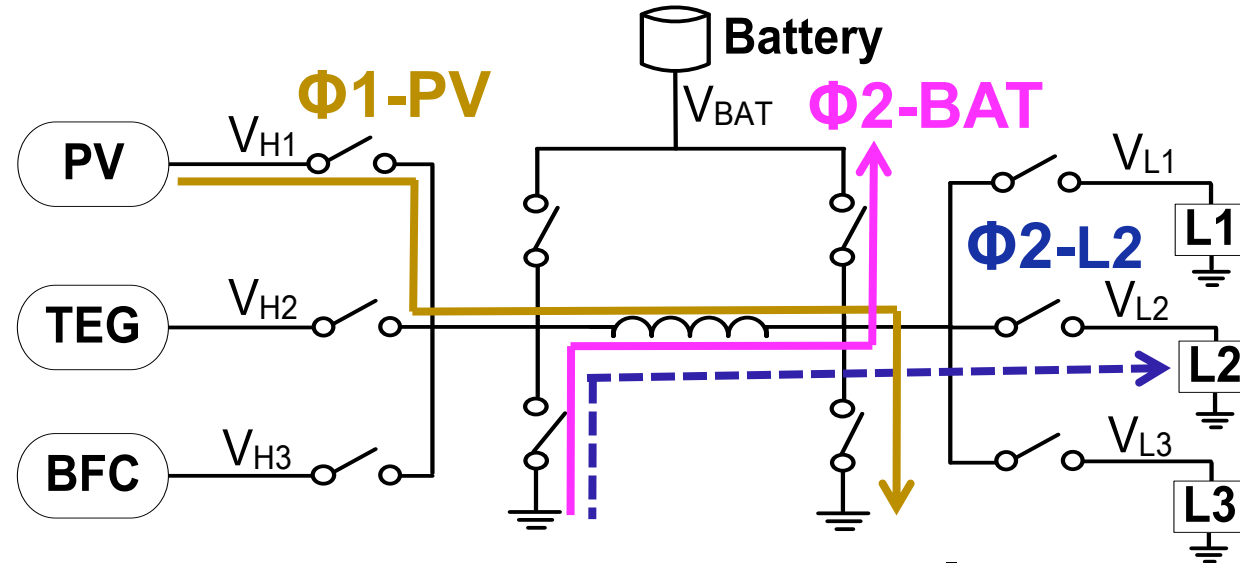
J. Kim et al., VLSI'11

C. Chae et al., ISSCC'07

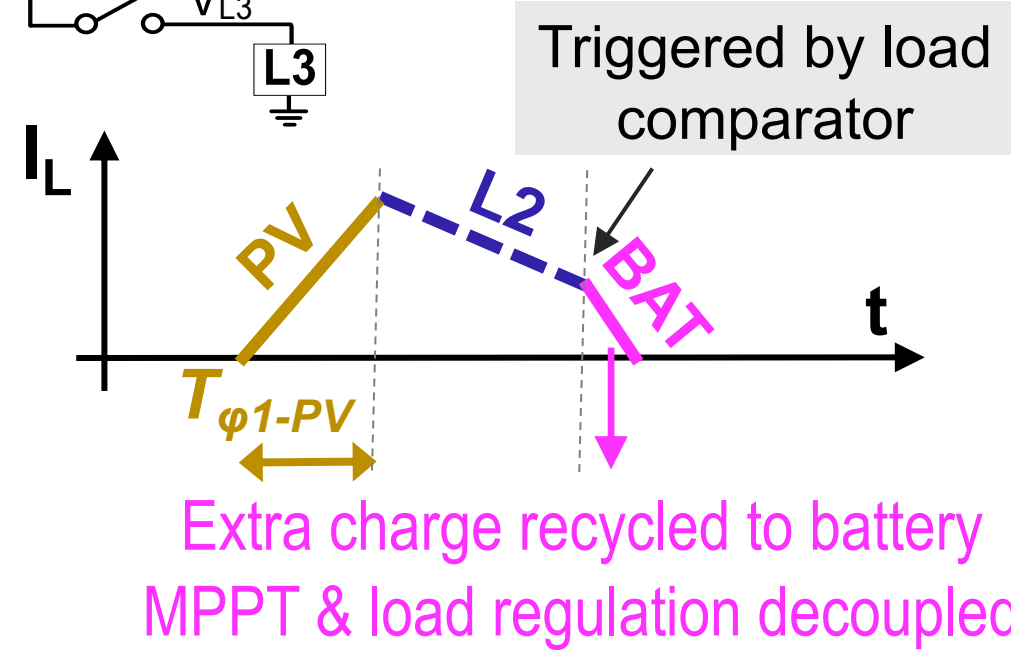
Outline

- State-of-the-Art and Single-Inductor Challenges
- **Decoupling Source MPPT and Load Regulation**
- Circuit Techniques for Wide Dynamic Range
- Measurement Results
- Conclusion

MPPT and Load Regulation Decoupling



Proposed

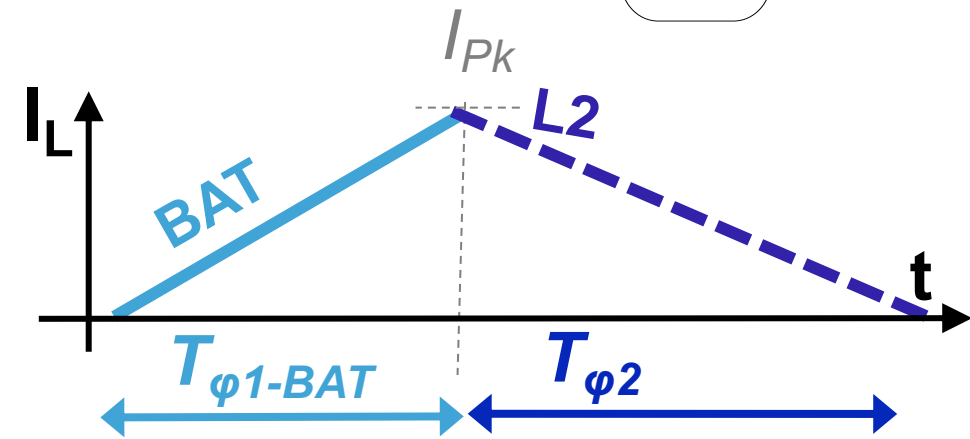
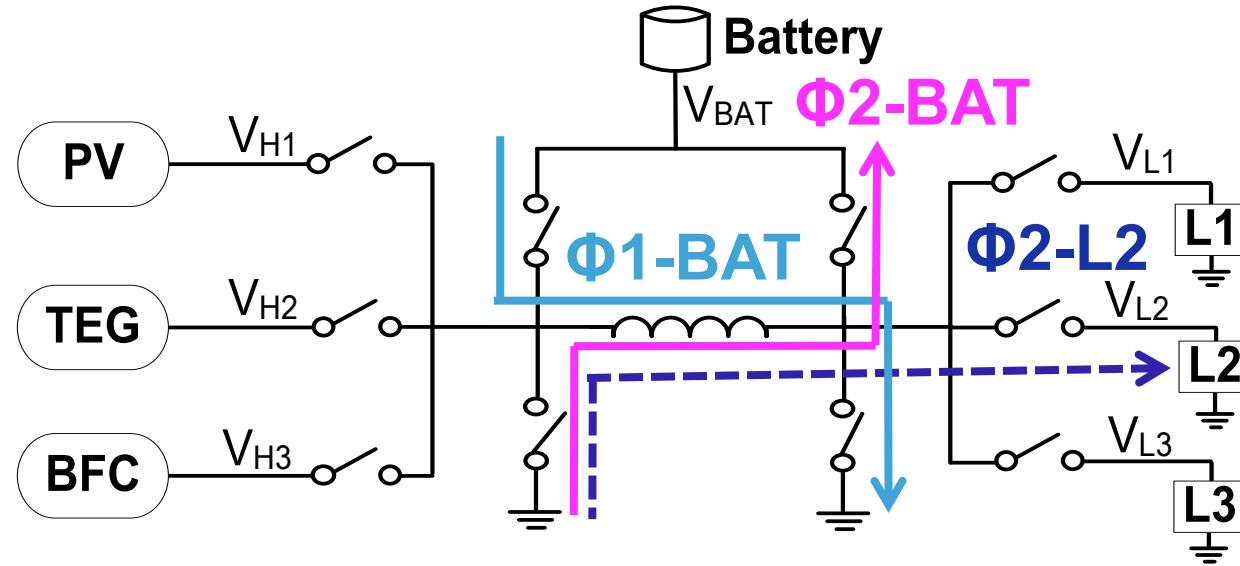


High voltage ripple
Degraded load regulation

Extra charge recycled to battery
MPPT & load regulation decoupled

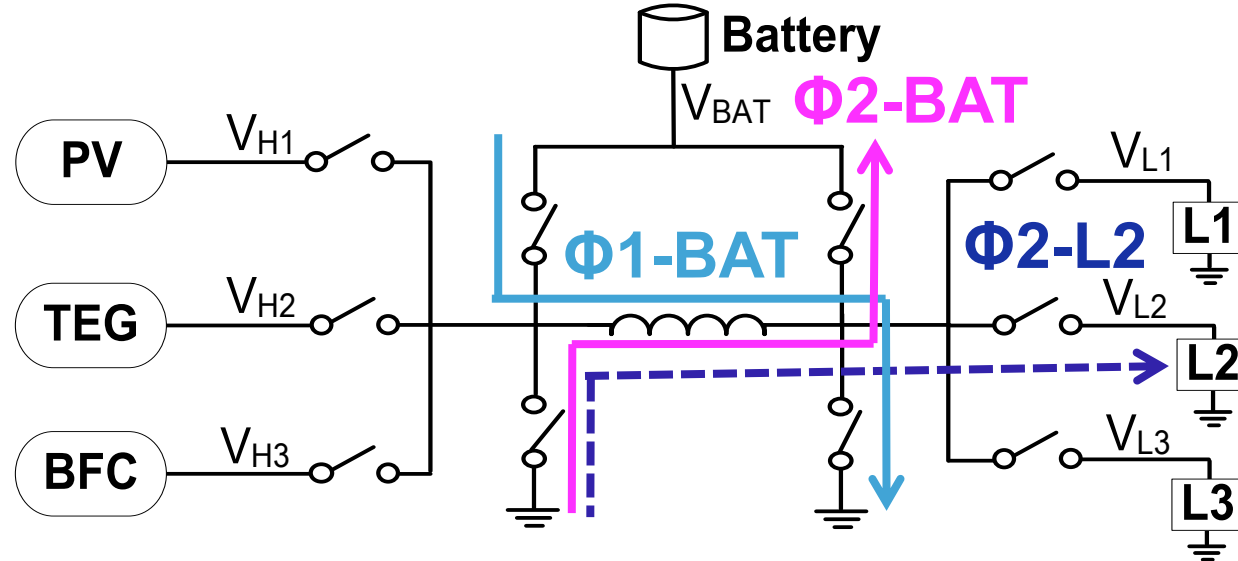
Trade off in "K. Chew et al., ISSCC 2013"

Battery-Inductor Charging Time ($T_{\phi 1-BAT}$) Calibration

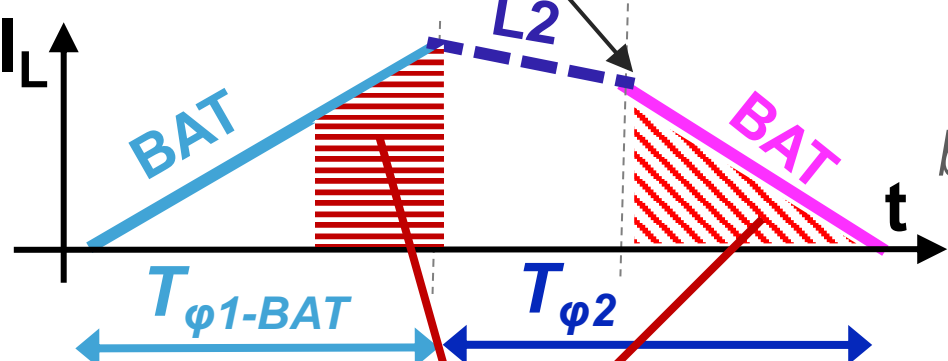


$T_{\phi 1-BAT}$ should be large enough to support the maximum load power

Battery-Inductor Charging Time ($T_{\phi 1-BAT}$) Calibration

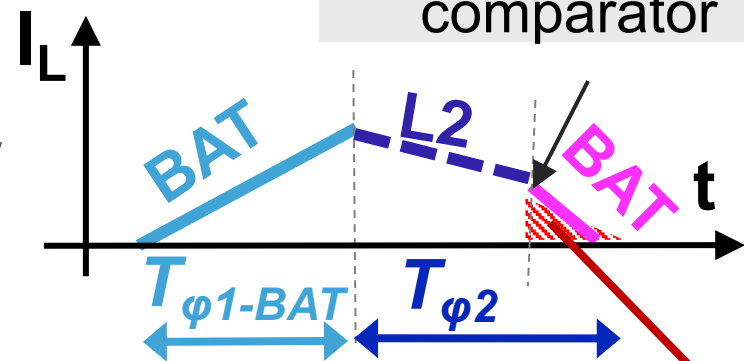


Triggered by load comparator



$T_{\phi 1-BAT}$ Calibration
based on load current indicator

J. Kim et al., VLSI'11



Conduction Losses

Free-up inductor time for energy harvesting by up to 10x

Minimize charge recycled back to battery

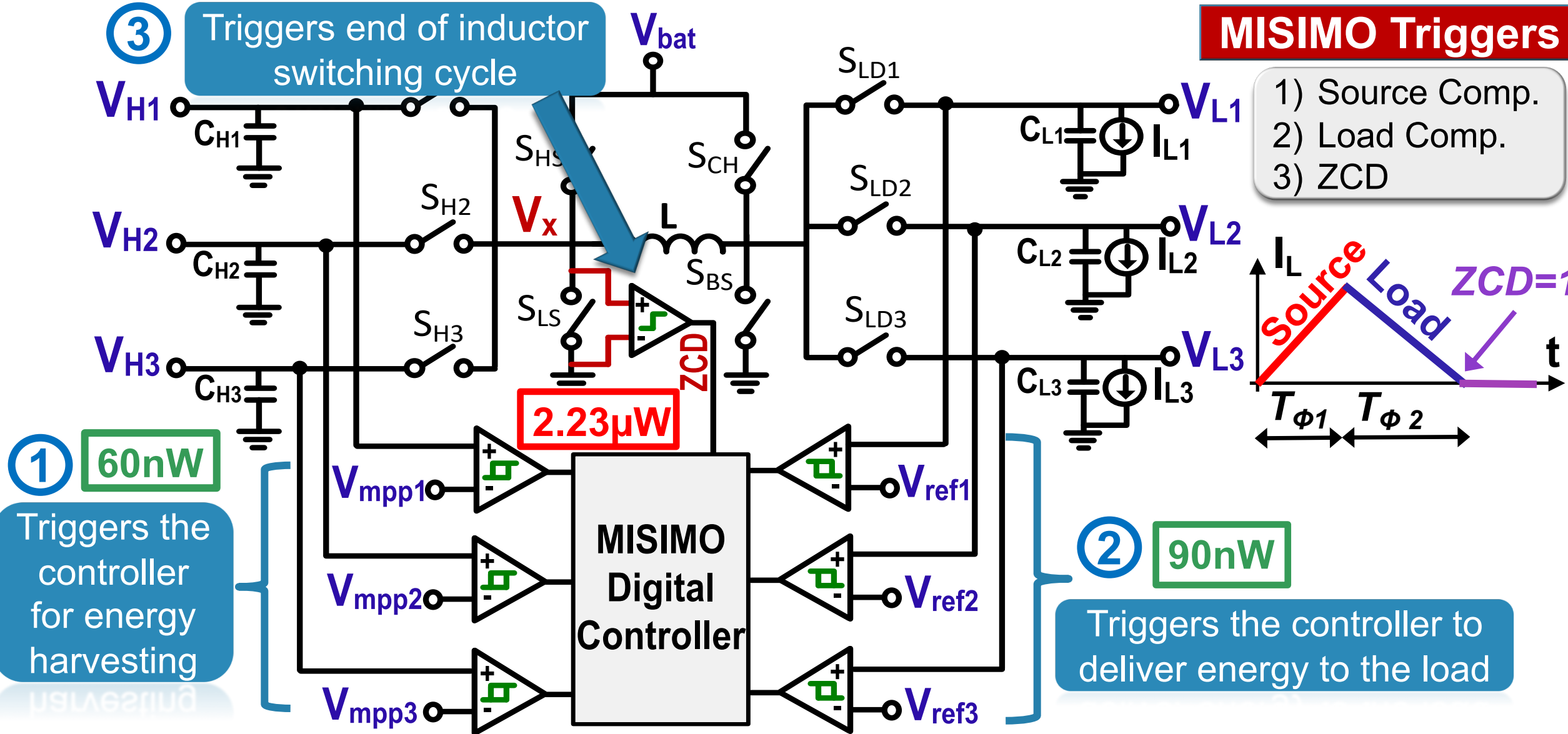
Outline

- State-of-the-Art and Single-Inductor Challenges
- Decoupling Source MPPT and Load Regulation
- **Circuit Techniques for Wide Dynamic Range**
- Measurement Results
- Conclusion

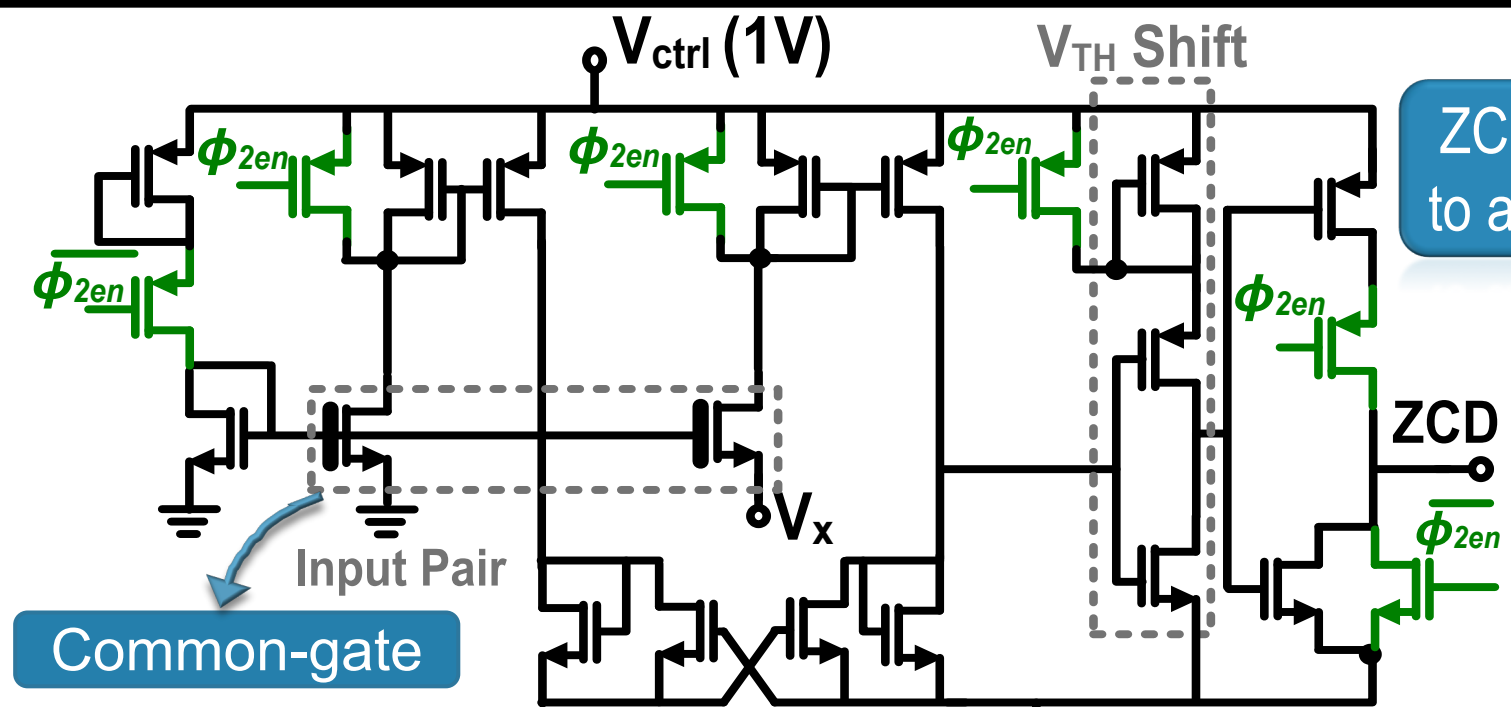
MISIMO Event Driven Controller

MISIMO Triggers

- 1) Source Comp.
- 2) Load Comp.
- 3) ZCD



Duty Cycled ZCD for Lowering Quiescent Power



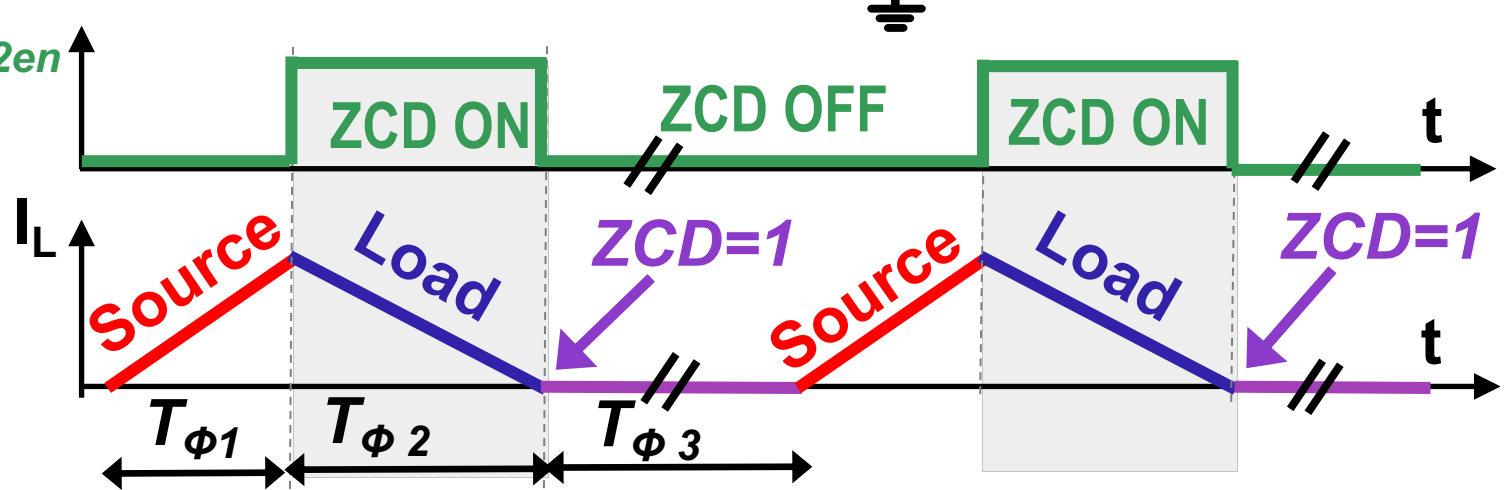
ZCD needs to be fast enough to avoid efficiency degradation

~~2.23 μ W~~

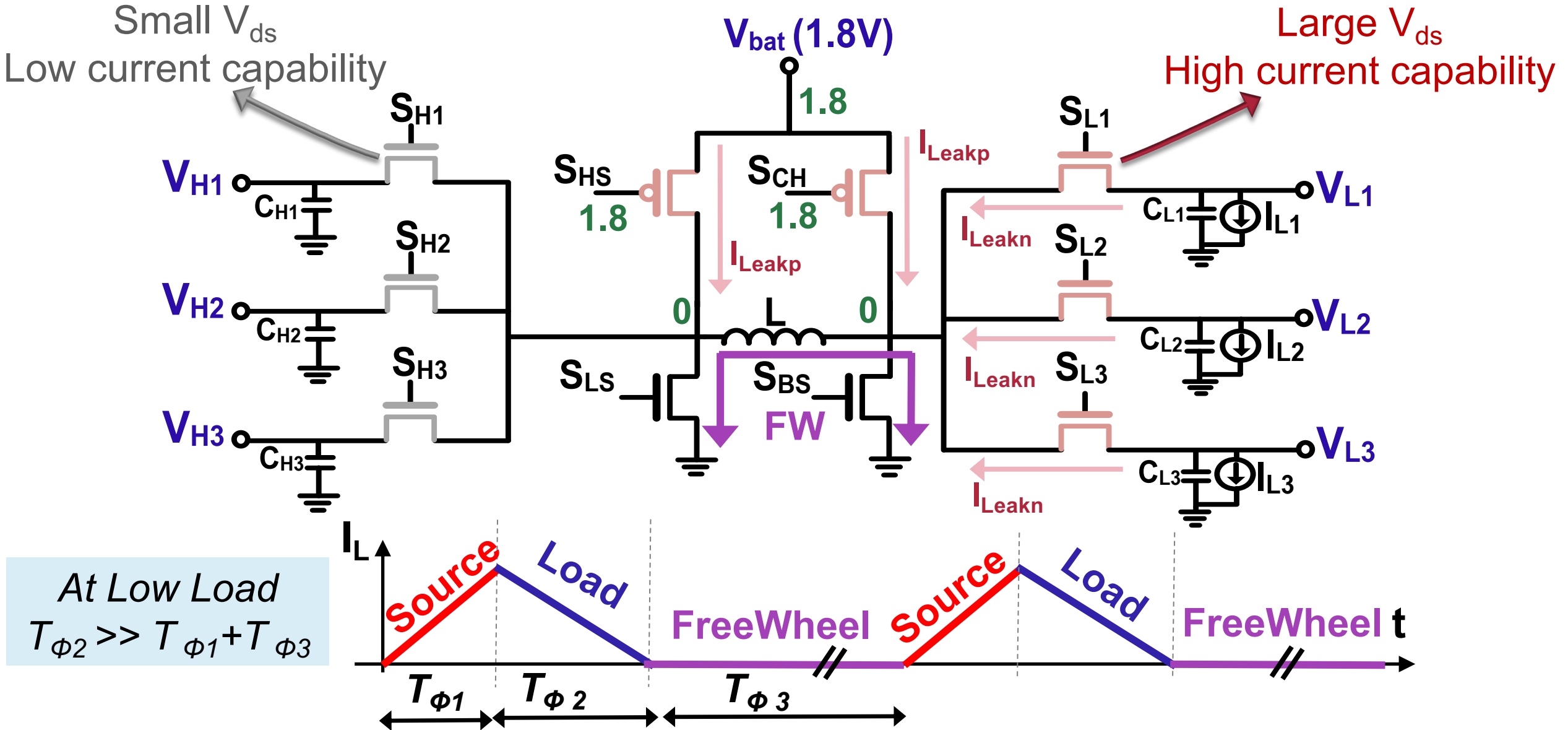
1nW @ $P_{out}=10\mu W$

Common-gate

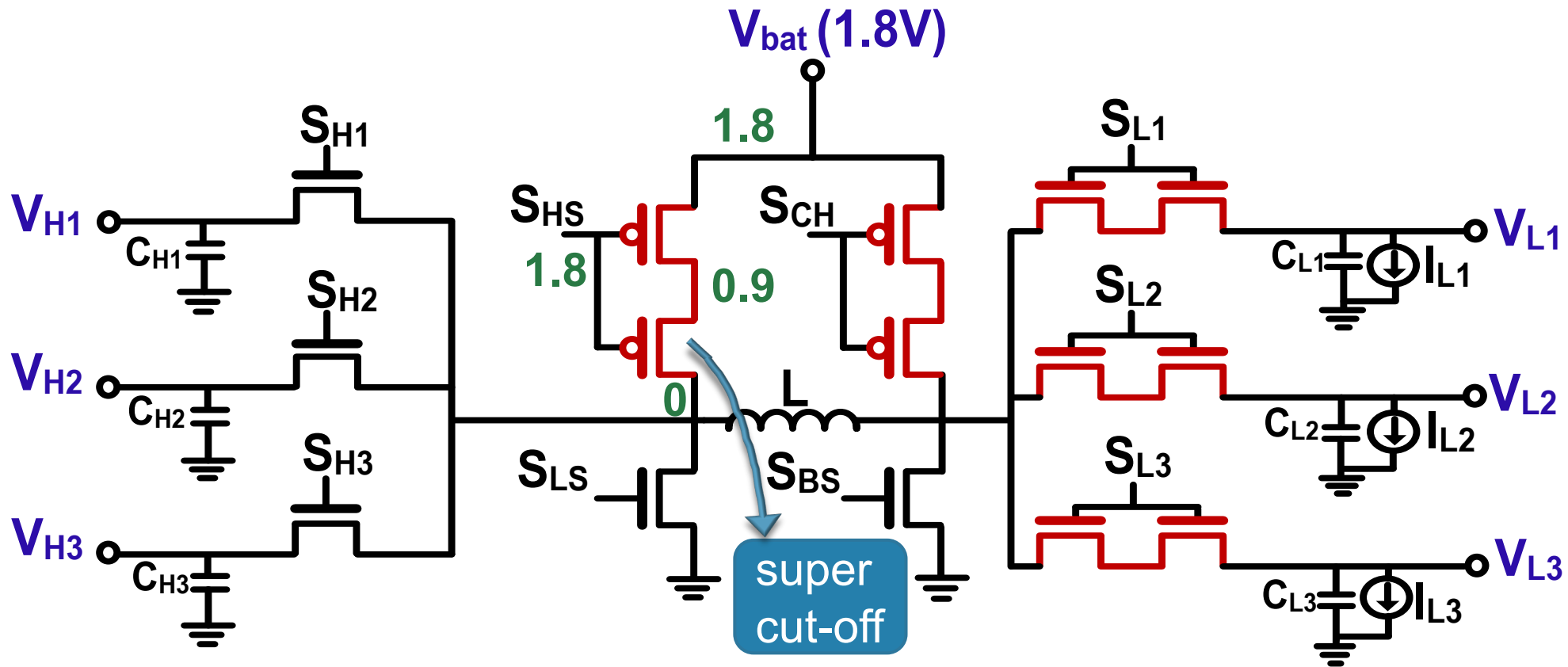
At Low Load
 $T_{\phi 2} \ll T_{\phi 1} + T_{\phi 3}$



Leakage Dominates Low Load Losses

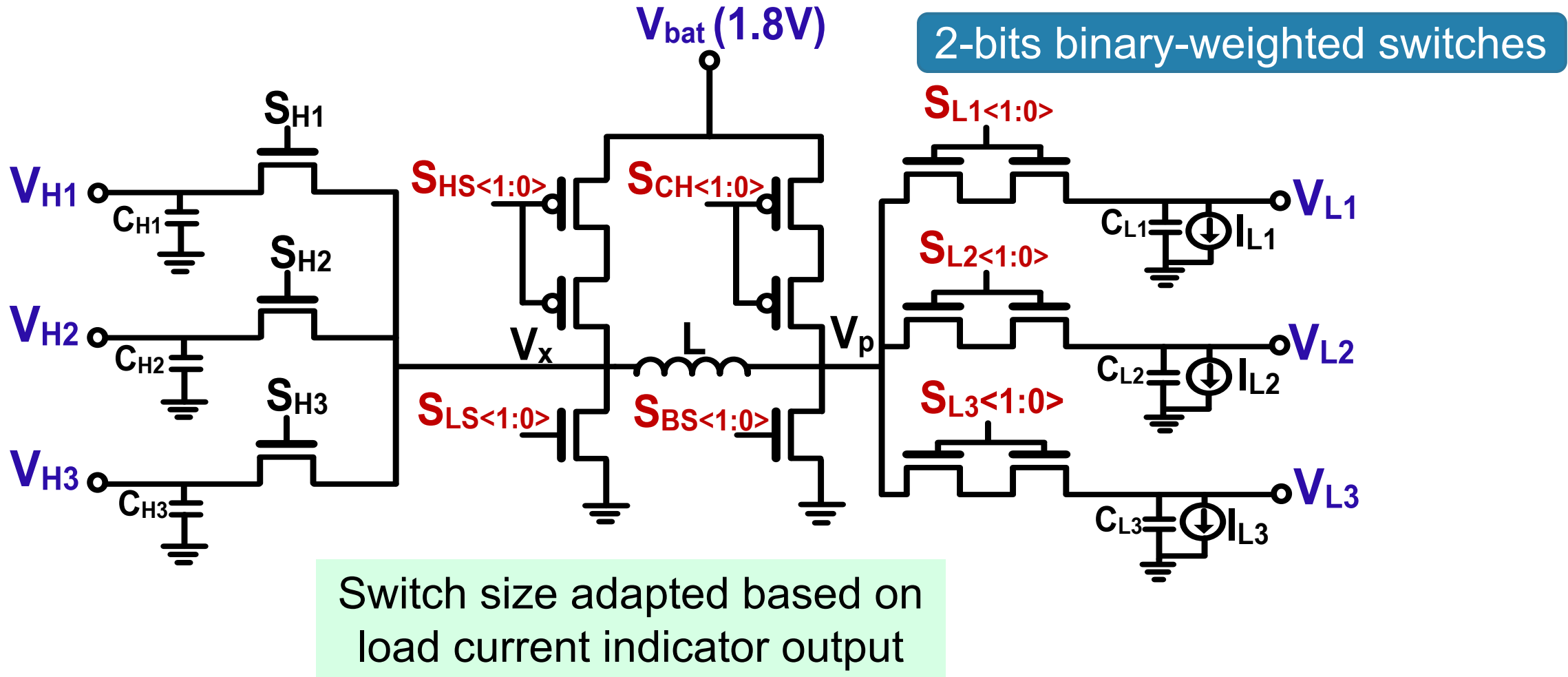


Cascoding Power Switches to Lower Leakage Losses



Cascoding transistors reduces leakage in freewheel phase by 9x

Switch Size Modulation (SSM)

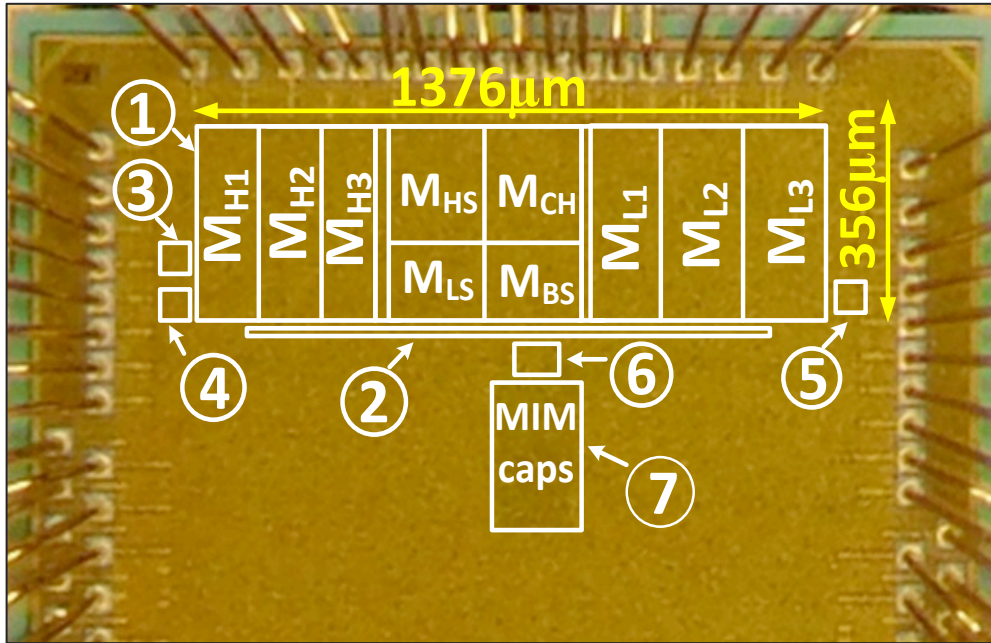


SSM reduces switching losses & improves efficiency by up to 24%

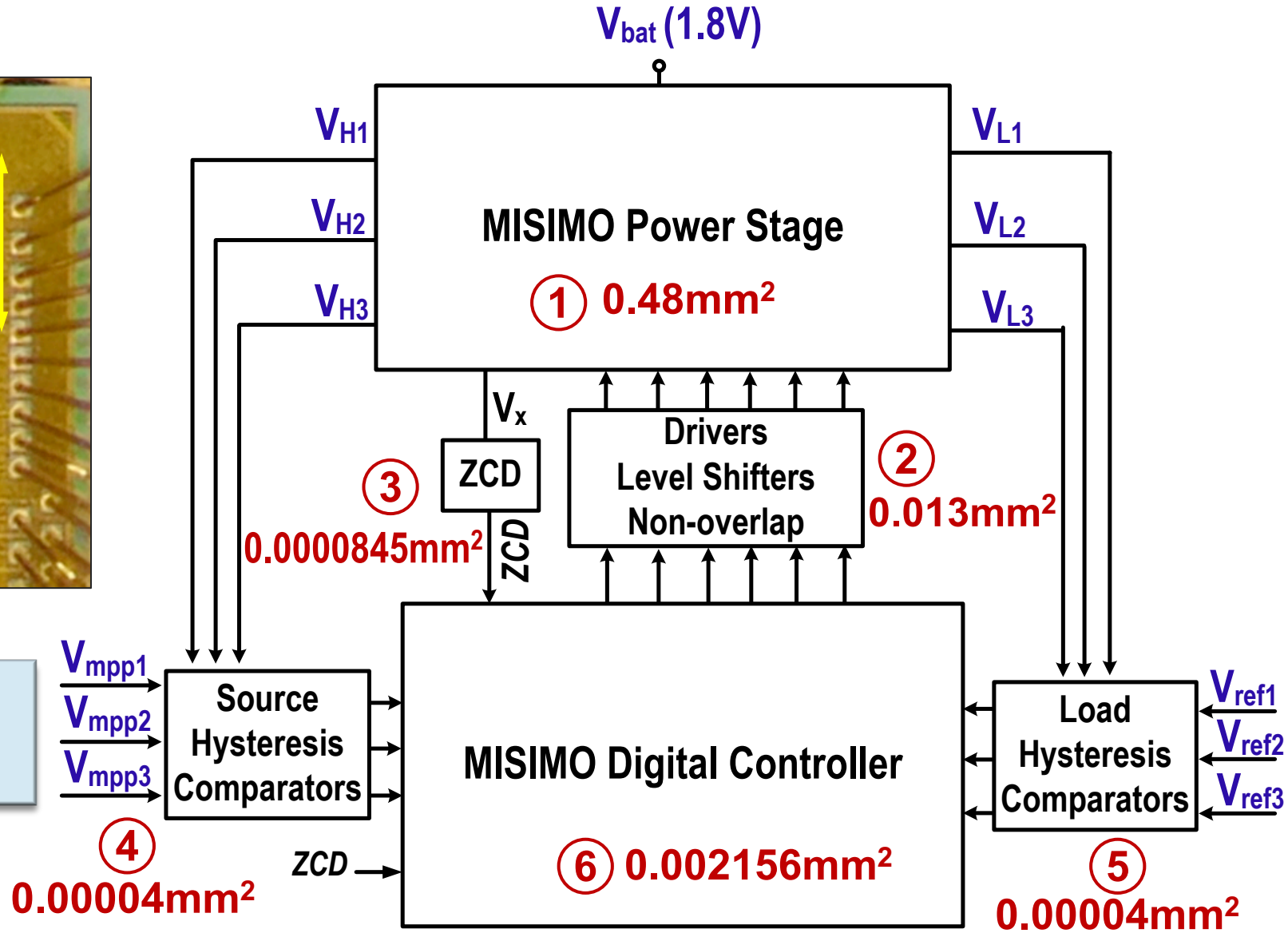
Outline

- State-of-the-Art and Single-Inductor Challenges
- Decoupling Source MPPT and Load Regulation
- Circuit Techniques for Wide Dynamic Range
- **Measurement Results**
- Conclusion

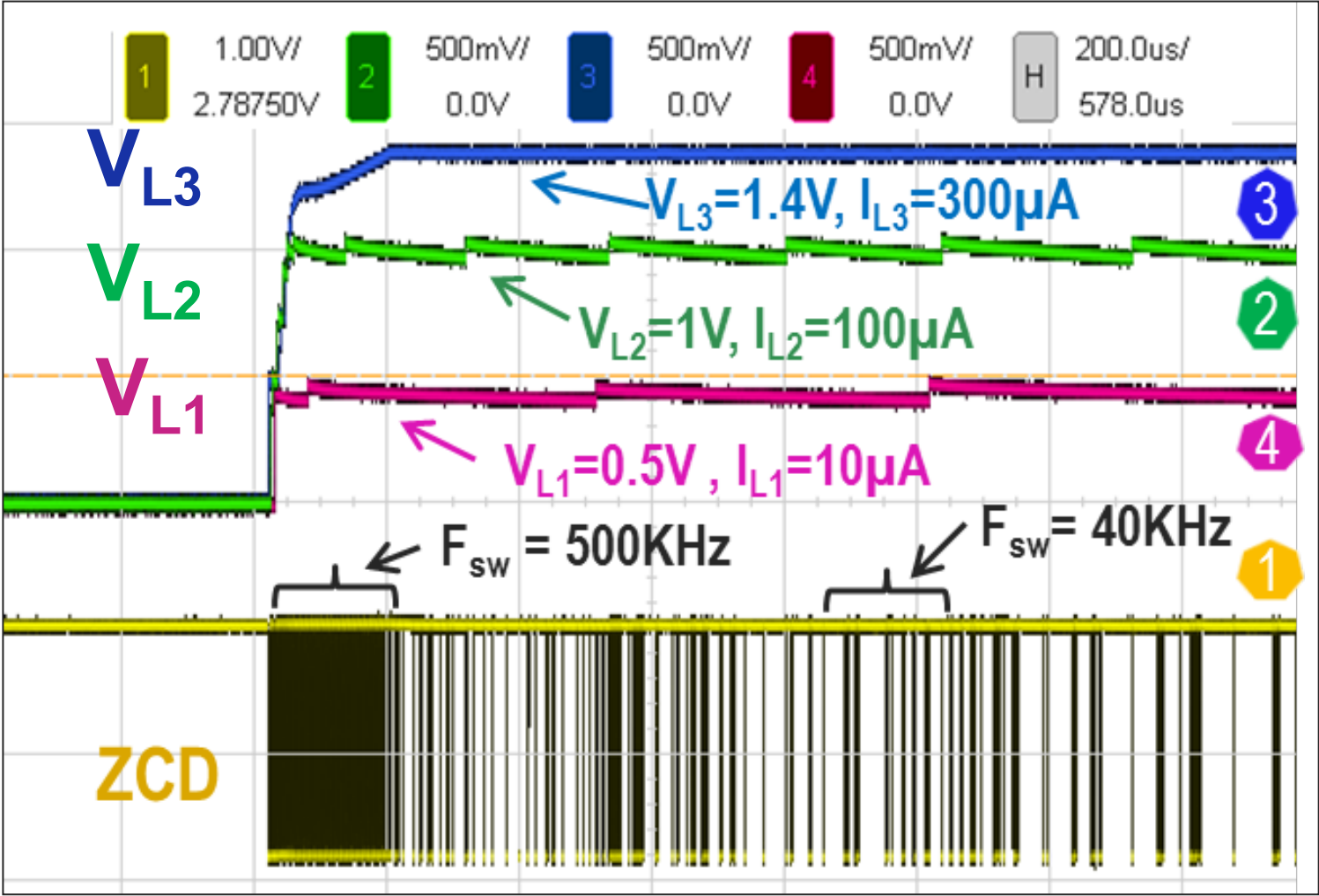
Die Micrograph



Implemented in 28nm FDSOI
Total Area = 0.5mm²

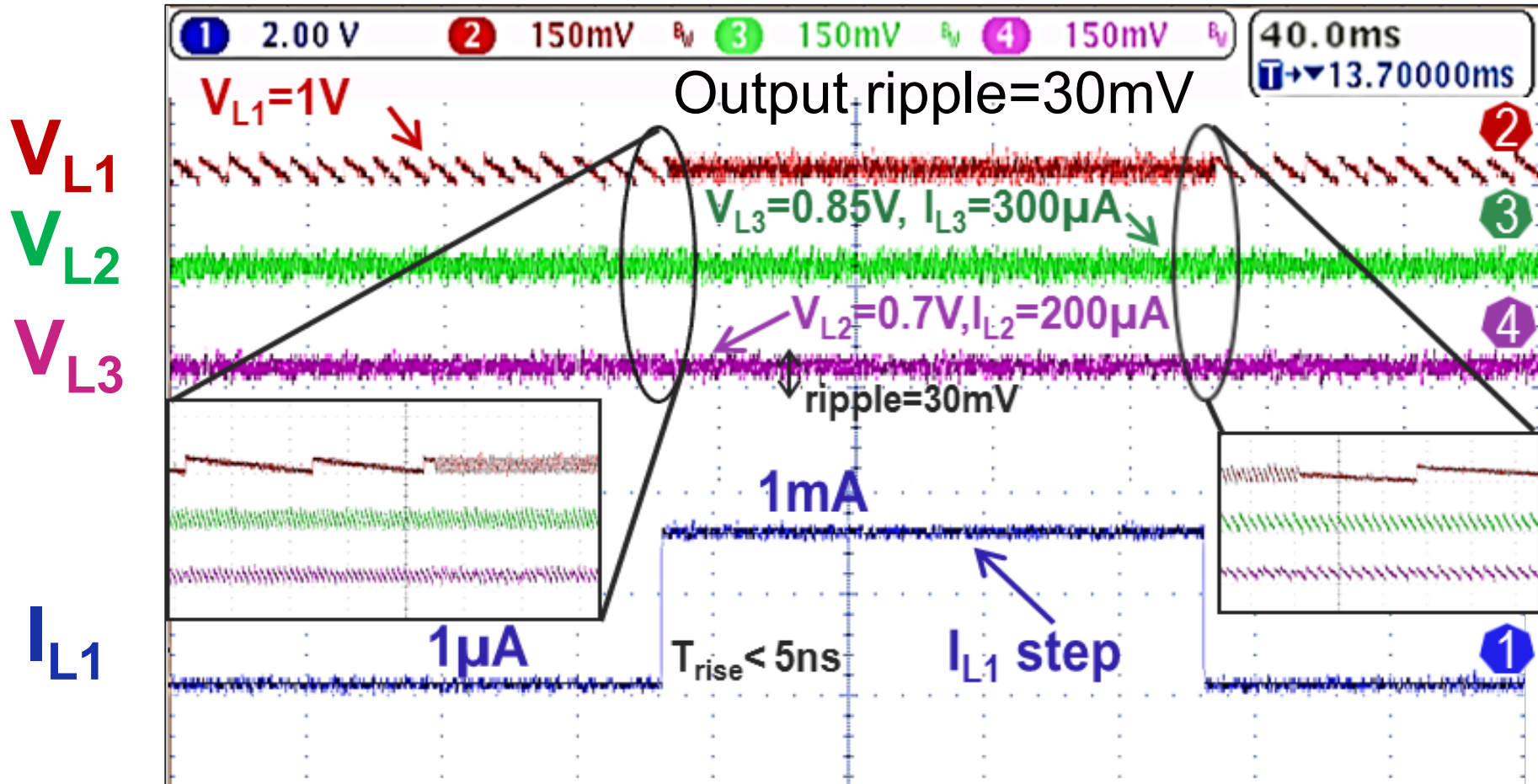


Measured Turn-On Transient Under Battery-Power



Measured turn-on transient demonstrates MISIMO PFM control

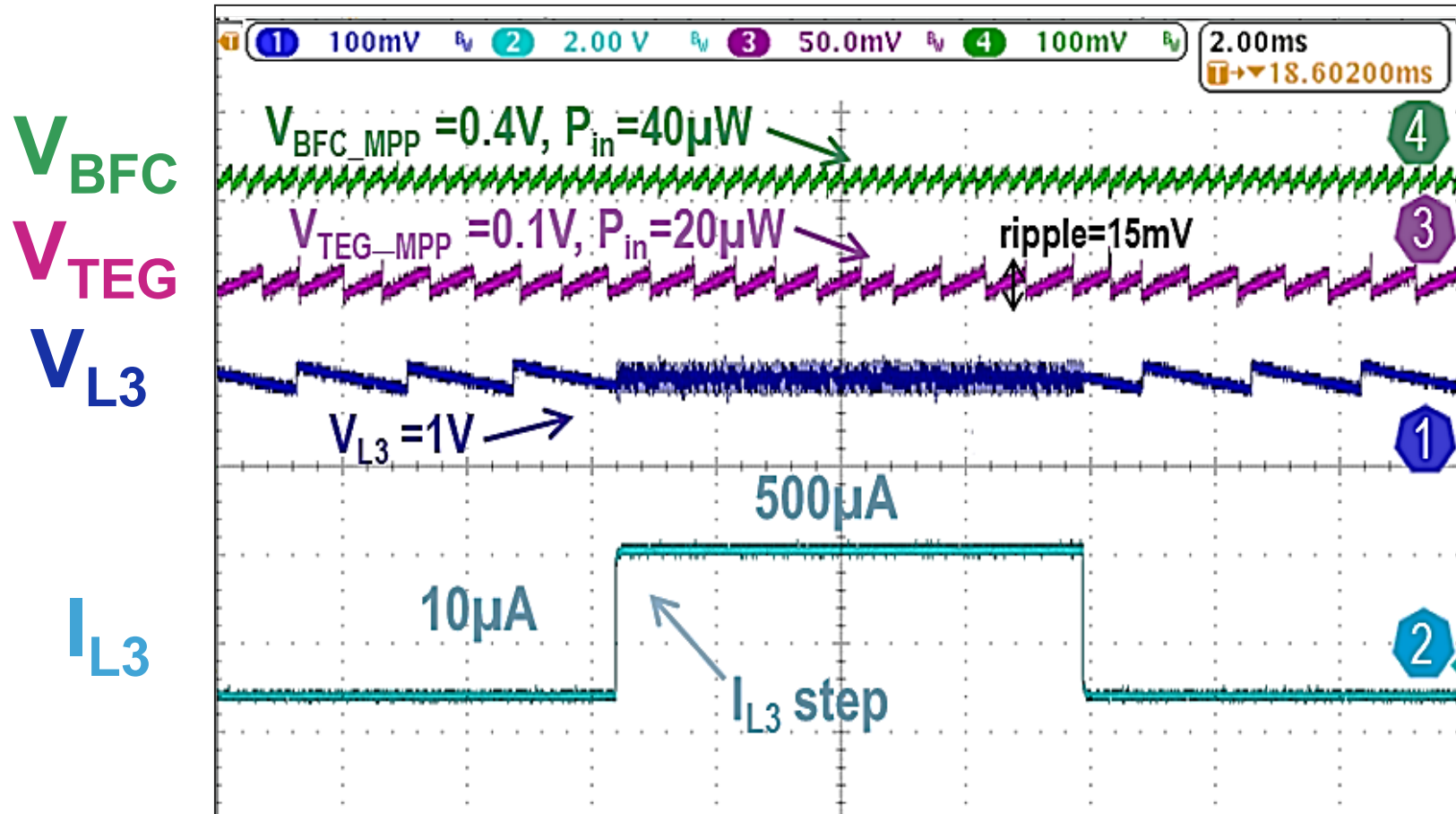
Measured Load1-Step Response



Ripple=30mV

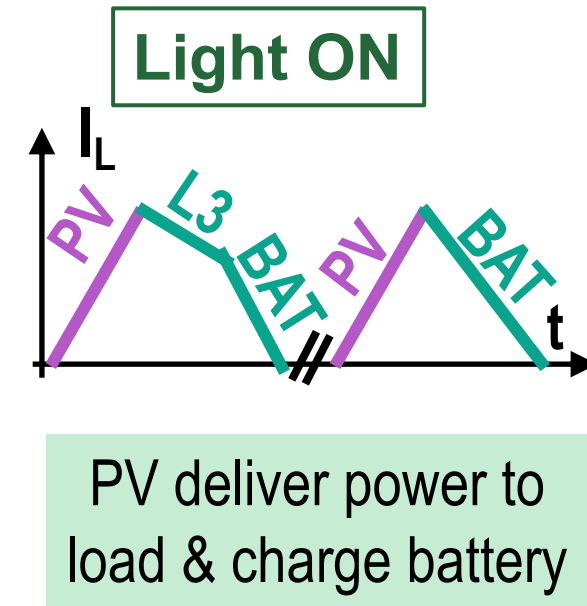
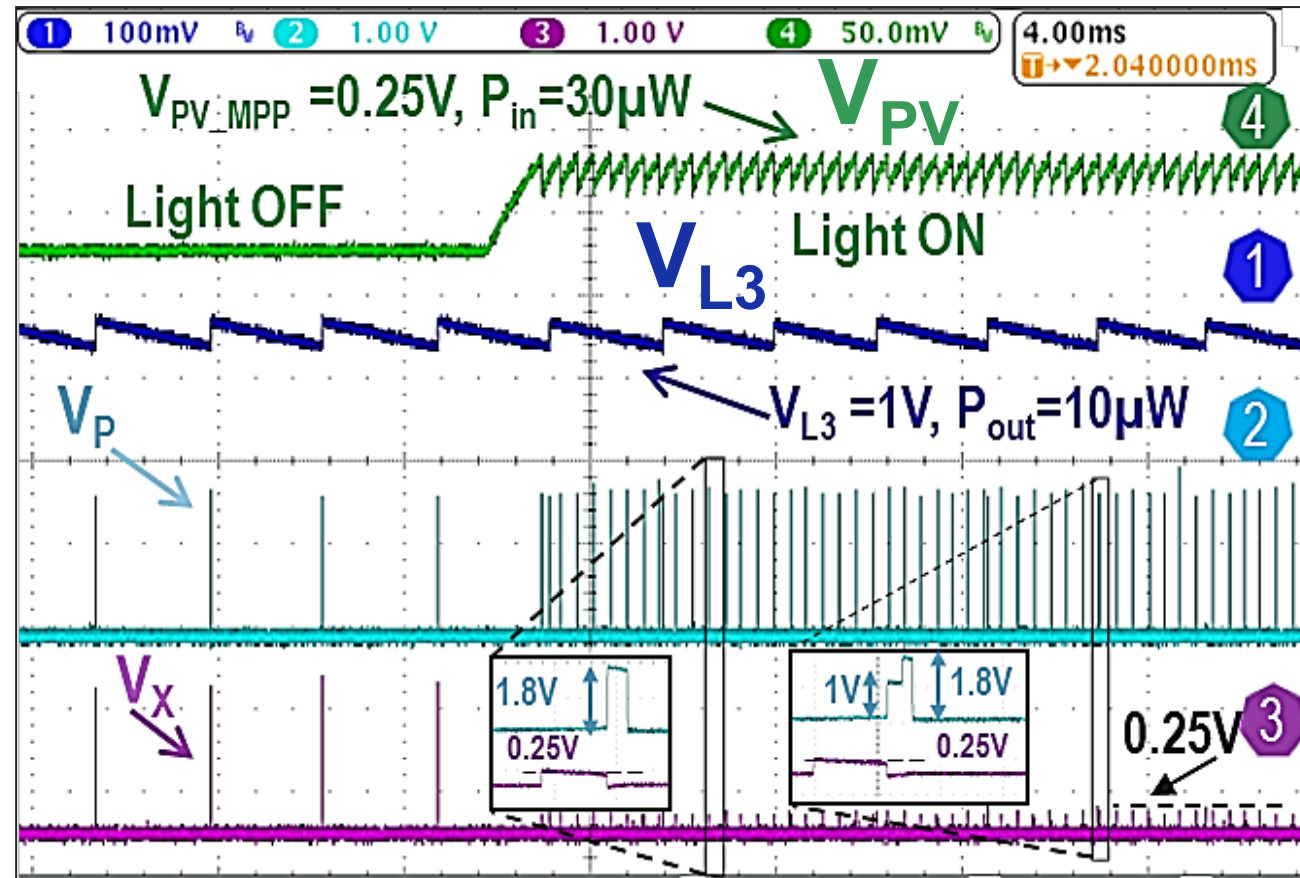
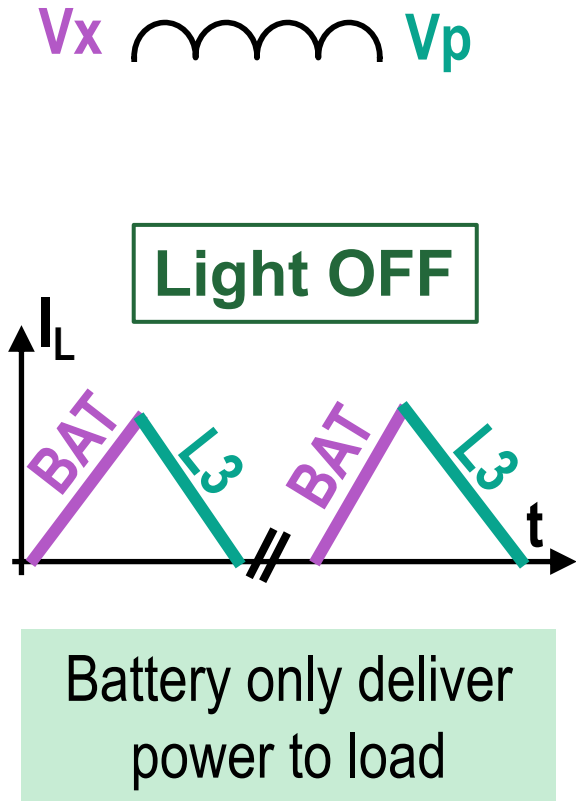
Measured L1 step demonstrates independent voltage regulation across 3 loads and negligible droop

Effect of Load Step on Source Regulation



Measured load step shows no effect on the simultaneous source regulation (for MPPT) and load regulation

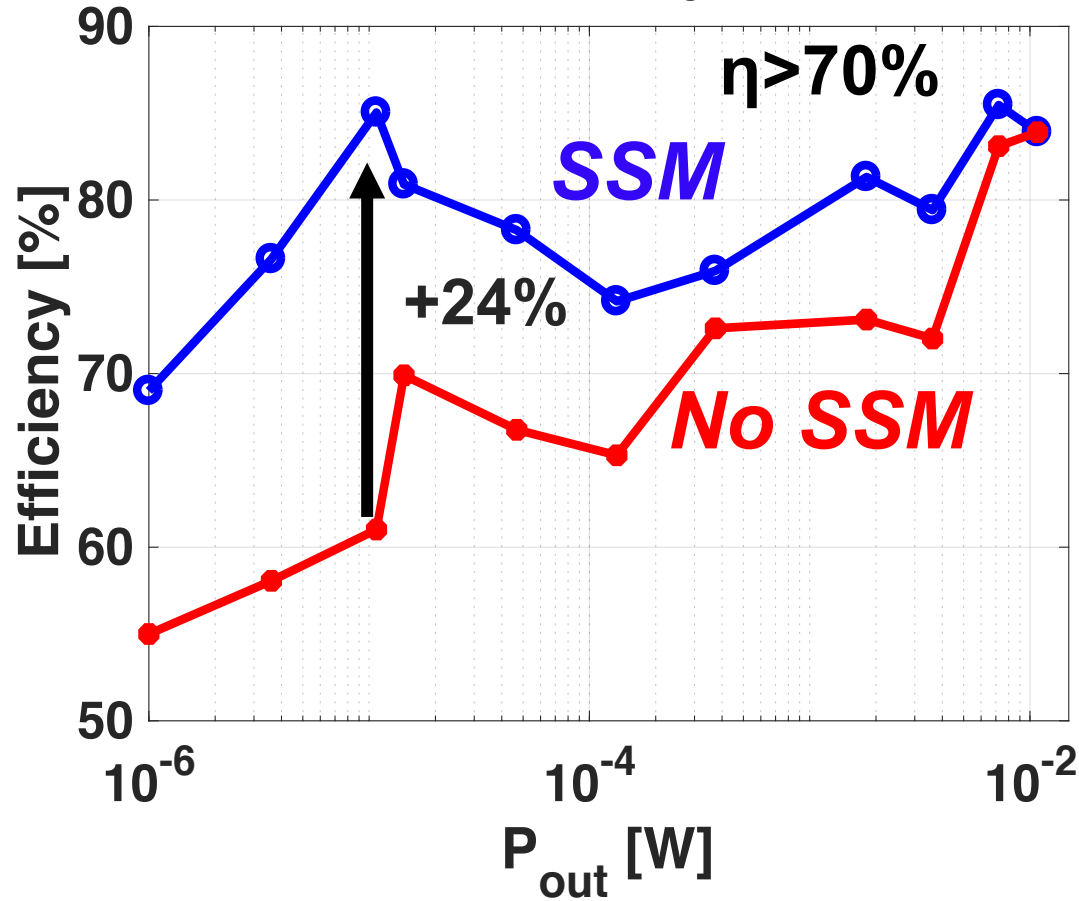
Measured Light-Step



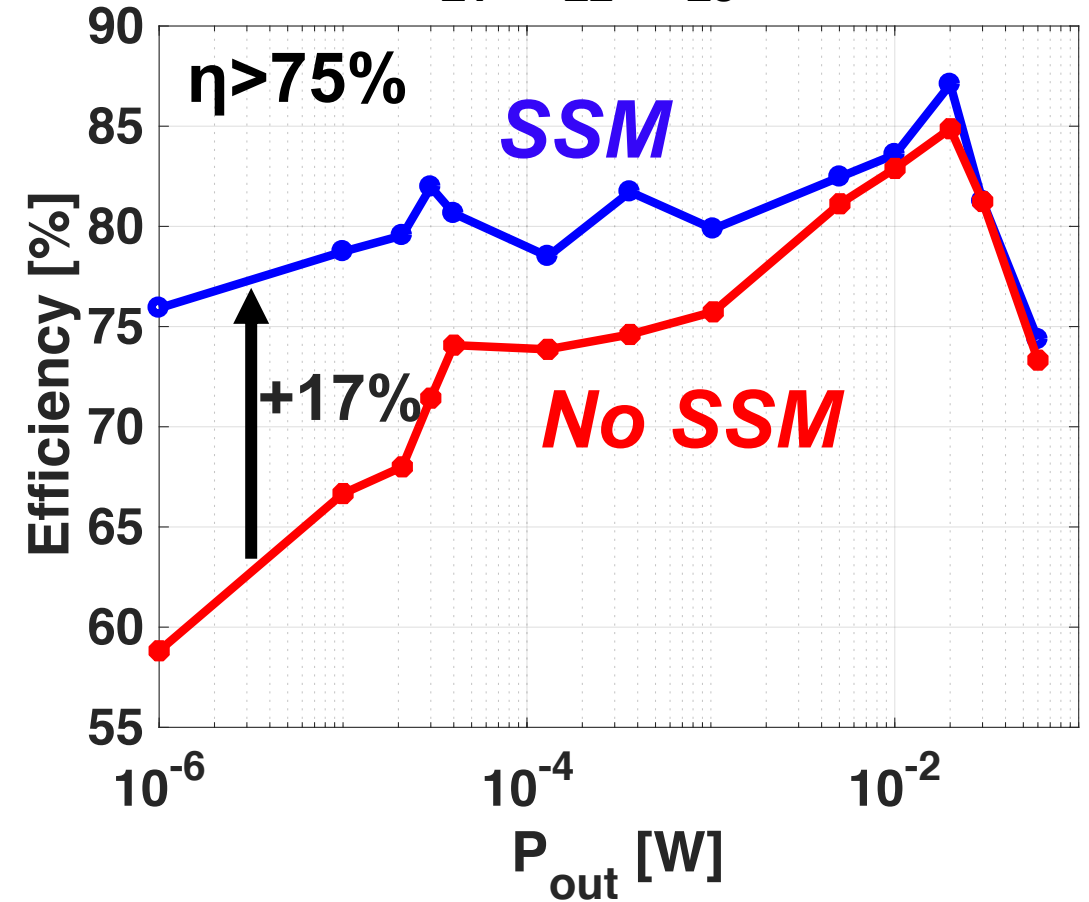
Measured light step demonstrates the capability of MISIMO to switch dynamically between different configurations

Effect of SSM on MISIMO Efficiency

$$V_{L1} = V_{L2} = V_{L3} = 0.6V$$

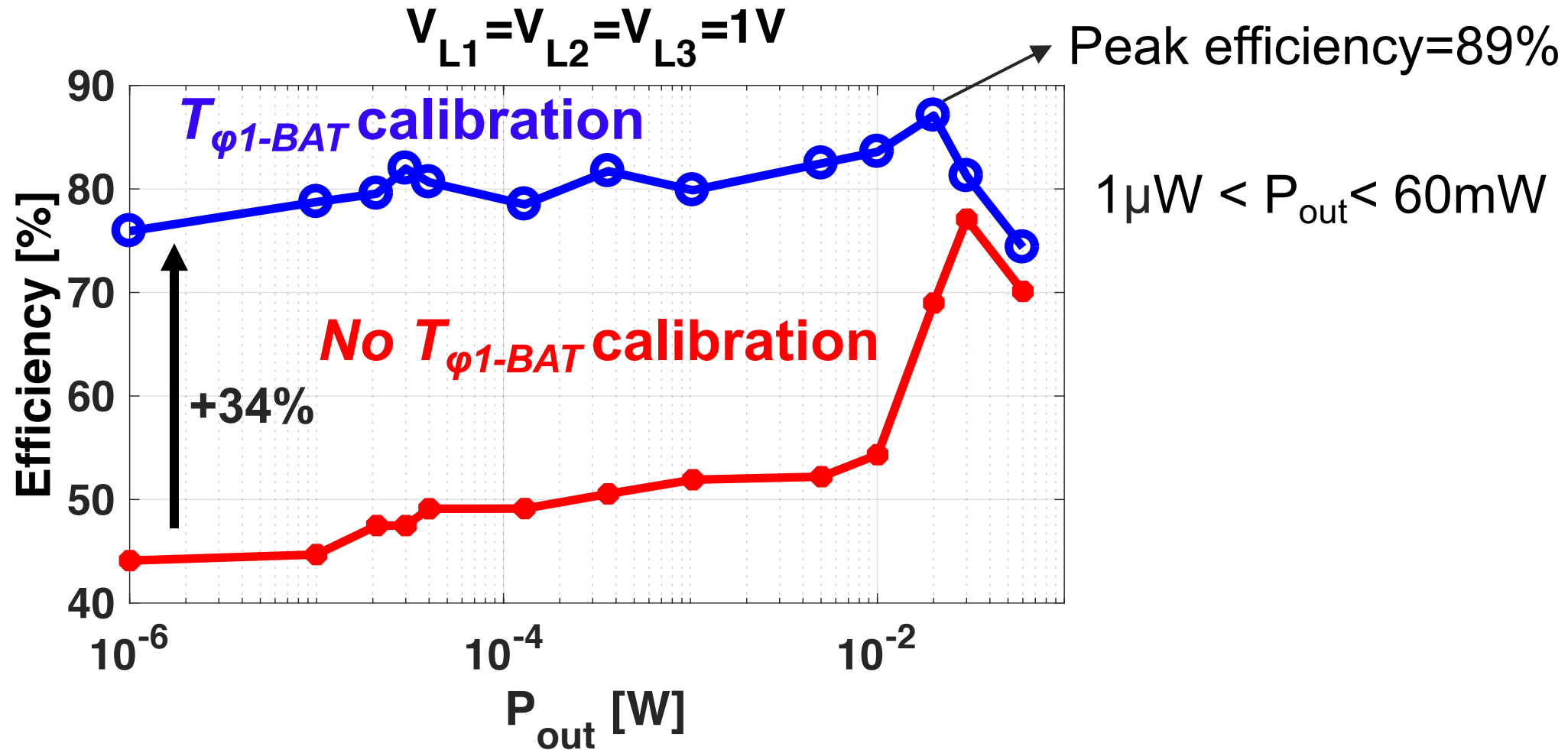


$$V_{L1} = V_{L2} = V_{L3} = 1V$$



SSM Improve MISIMO Efficiency by up to 24%

Effect of $T_{\phi 1-BAT}$ Calibration on MISIMO Efficiency



$T_{\phi 1-BAT}$ calibration improve MISIMO efficiency by up to 34%

Comparison to State-of-Art

	Bandyopadhyay, JSSC'12	K. Chew ISSCC'13	Shrivastava, VLSI'14	Chen, ISSCC'15	Chowdary, JSSC'16	This Work
Technology	0.35 μ m	0.18 μ m	0.13 μ m	0.5 μ m	0.18 μ m	28nm FDSOI
No of inputs	3+battery	1+battery	1+battery	1+battery	3+supercap	3+battery
No of outputs	1+battery	2+battery	3+battery	1+battery	1+supercap	3+battery
Converter Architecture	2-stage, 1-ind Buck/Boost	1 stage, 1-ind Buck-Boost	2-stage, 1-ind Buck/Boost	1-stage, 1-ind Buck/Boost	2-stage, 1-ind Buck-Boost	1-stage, 1-ind Buck-Boost
Load regulation mechanism	PFM	PFM	PFM I_{PK} Control	PFM	PFM	PFM+PWM +SSM
MPPT mechanism	Adaptive T_{ON} Fixed F_{SW}	Constant T_{ON} Vary F_{SW}	Constant T_{ON} Vary F_{SW}	Constant T_{ON} Vary F_{SW}	Constant I_{PK} Vary F_{SW}	Adaptive T_{ON} Adaptive F_{SW}
L	22 μ H	10 μ	20 μ H	4.7 μ H	47 μ H	10 μ H
Die Area (mm²)	~15	4.62	2.25	0.5	1.1	0.5
V_{out} (V)	1.8V	1V, 1.8V	1.2, 1.5, 3.3V	1~3.3V	1.2V~1.8V	0.4~1.4V
Quiescent P/I	2.7 μ A@ V_{DD} =1.8V	0.4 μ A@ V_{DD} =1V	1.2 μ W	1 μ A@ V_{DD} =4V	18nA	262nW
P_{out}	9 μ W~540 μ W	1 μ W ~ 10mW	<100mW	1 μ W~15mW	60nW~40 μ W [‡]	1μW~60mW
Dynamic Range (DR) for η>70%	60X	10,000X	16,500X [‡]	15,000X	667X [‡]	60,000X
Peak Efficiency	90%	83%	92%	93%	87%	89%

Comparison to State-of-Art

	Bandyopadhyay, JSSC'12	K. Chew ISSCC'13	Shrivastava, VLSI'14	Chen, ISSCC'15	Chowdary, JSSC'16	This Work
Technology	0.35 μ m	0.18 μ m	0.13 μ m	0.5 μ m	0.18 μ m	28nm FDSOI
No of inputs	3+battery	1+battery	1+battery	1+battery	3+supercap	3+battery
No of outputs	1+battery	2+battery	3+battery	1+battery	1+supercap	3+battery
Converter Architecture	2-stage, 1-ind Buck/Boost	1 stage, 1-ind Buck-Boost	2-stage, 1-ind Buck/Boost	1-stage, 1-ind Buck/Boost	2-stage, 1-ind Buck-Boost	1-stage, 1-ind Buck-Boost
Load regulation mechanism	PFM	PFM	PFM I_{PK} Control	PFM	PFM	PFM+PWM +SSM
MPPT mechanism	Adaptive T_{ON} Fixed F_{SW}	Constant T_{ON} Vary F_{SW}	Constant T_{ON} Vary F_{SW}	Constant T_{ON} Vary F_{SW}	Constant I_{PK} Vary F_{SW}	Adaptive T_{ON} Adaptive F_{SW}
L	22 μ H	10 μ	20 μ H	4.7 μ H	47 μ H	10 μ H
Die Area (mm²)	~15	4.62	2.25	0.5	1.1	0.5
V_{out} (V)	1.8V	1V, 1.8V	1.2, 1.5, 3.3V	1~3.3V	1.2V~1.8V	0.4~1.4V
Quiescent P/I	2.7 μ A@ V_{DD} =1.8V	0.4 μ A@ V_{DD} =1V	1.2 μ W	1 μ A@ V_{DD} =4V	18nA	262nW
P_{out}	9 μ W~540 μ W	1 μ W ~ 10mW	<100mW	1 μ W~15mW	60nW~40 μ W [‡]	1μW~60mW
Dynamic Range (DR) for η>70%	60X	10,000X	16,500X [‡]	15,000X	667X [‡]	60,000X
Peak Efficiency	90%	83%	92%	93%	87%	89%

Comparison to State-of-Art

	Bandyopadhyay, JSSC'12	K. Chew ISSCC'13	Shrivastava, VLSI'14	Chen, ISSCC'15	Chowdary, JSSC'16	This Work
Technology	0.35 μ m	0.18 μ m	0.13 μ m	0.5 μ m	0.18 μ m	28nm FDSOI
No of inputs	3+battery	1+battery	1+battery	1+battery	3+supercap	3+battery
No of outputs	1+battery	2+battery	3+battery	1+battery	1+supercap	3+battery
Converter Architecture	2-stage, 1-ind Buck/Boost	1 stage, 1-ind Buck-Boost	2-stage, 1-ind Buck/Boost	1-stage, 1-ind Buck/Boost	2-stage, 1-ind Buck-Boost	1-stage, 1-ind Buck-Boost
Load regulation mechanism	PFM	PFM	PFM I_{PK} Control	PFM	PFM	PFM+PWM +SSM
MPPT mechanism	Adaptive T_{ON} Fixed F_{SW}	Constant T_{ON} Vary F_{SW}	Constant T_{ON} Vary F_{SW}	Constant T_{ON} Vary F_{SW}	Constant I_{PK} Vary F_{SW}	Adaptive T_{ON} Adaptive F_{SW}
L	22 μ H	10 μ	20 μ H	4.7 μ H	47 μ H	10 μ H
Die Area (mm²)	~15	4.62	2.25	0.5	1.1	0.5
V_{out} (V)	1.8V	1V, 1.8V	1.2, 1.5, 3.3V	1~3.3V	1.2V~1.8V	0.4~1.4V
Quiescent P/I	2.7 μ A@ V_{DD} =1.8V	0.4 μ A@ V_{DD} =1V	1.2 μ W	1 μ A@ V_{DD} =4V	18nA	262nW
P_{out}	9 μ W~540 μ W	1 μ W ~ 10mW	<100mW	1 μ W~15mW	60nW~40 μ W \ddagger	1μW~60mW
Dynamic Range (DR) for η>70%	60X	10,000X	16,500X \ddagger	15,000X	667X \ddagger	60,000X
Peak Efficiency	90%	83%	92%	93%	87%	89%

Outline

- State-of-the-Art and Single-Inductor Challenges
- Decoupling Source MPPT and Load Regulation
- Circuit Techniques for Wide Dynamic Range
- Measurement Results
- **Conclusion**

Conclusion

- Small form factor MISIMO architecture enabled by techniques that decouple the source side 2-D MPPT and load side regulation
- MISIMO achieves $\eta_{pk} = 89\%$ and $\eta \geq 70\%$ across $1\mu W < P_{out} < 60mW$ by employing efficiency enhancement techniques including:
 - Switch Size Modulation (SSM) [improve efficiency by up to 24%]
 - $T_{\phi 1-BAT}$ calibration (PWM) [improve efficiency by up to 34%]
 - Cascoded PS switch-structure [reduce leakage by 9x]
 - Duty-cycled ZCD [reduce P_Q by >2000x]